Dietary nucleotides can prevent glucocorticoid-induced telomere attrition in a fast-growing wild vertebrate

Stefania Casagrande[1*], Jasmine L. Loveland[2], Marlene Oefele[1] , Winnie Boner[3], Sara Lupi[4], Antoine Stier[5,6], and Michaela Hau[1,7]

1. Max Planck Institute for Biological Intelligence, Evolutionary Physiology Group, 82319 Seewiesen, Germany.
2. Department of Cognitive and Behavioral Biology, University of Vienna, 1030 Vienna, Austria
3. Institute of Biodiversity Animal Health and Comparative Medicine, University of Glasgow, Glasgow, G12 8QQ, UK.
4. Konrad Lorenz Institute of Ethology, Savoyenstrasse 1a, 1160 Vienna, Austria
5. Université de Strasbourg, CNRS, Institut Pluridisciplinaire Hubert Curien, UMR7178, 67000 Strasbourg, France
6. Department of Biology, University of Turku, FI-20014 Turku, Finland
7. Department of Biology, University of Konstanz, D-78464 Konstanz, Germany.

*Author for correspondence (stefania.casagrande@bi.mpg.de)

Abstract

Telomeres are chromosome protectors that shorten during cell replication and in stressful conditions. Developing individuals are susceptible to telomere erosion when their growth is fast and resources are limited. This is critical because the rate of telomere attrition in early life is linked to health and life span of adults. The metabolic telomere attrition hypothesis (MeTA) suggests that telomere dynamics can respond to biochemical signals conveying information about the organism's energetic state. Among these signals are glucocorticoids – hormones that promote catabolic processes, potentially impairing costly telomere maintenance – and nucleotides, which activate anabolic pathways through the cellular enzyme target of rapamycin (TOR), thus preventing telomere attrition. During the energetically demanding growth phase, the regulation of telomeres in response to two contrasting signals—one promoting telomere maintenance and the other attrition—provides an ideal experimental setting to test the MeTa. We studied nestlings of a rapidly developing free-living passerine, the great tit (*Parus major*), that either received glucocorticoids (Cort-chicks), nucleotides (Nuc-chicks), or a combination of both (NucCort-chicks), comparing these with controls (Cnt-chicks). As expected, Cort-chicks showed telomere attrition, while NucCort-chicks did not. NucCort-chicks was the only group showing increased gene expression of *telo2* (a proxy for TOR activation), of mitochondrial enzymes linked to ATP production (*atp5f1a, atp5f1b, cox6a1, cox4*) and a higher efficiency in aerobically producing ATP. NucCort-chicks had also a higher expression of telomere maintenance genes (*terf2*) and of enzymatic antioxidant genes (*gpx4-sod1*). The findings show that nucleotide availability is crucial for preventing telomere erosion during fast growth in stressful environments.

Introduction

Growth is a delicate life-history stage, where new cells and tissues are produced at a very high rate. It involves an increase in body mass that requires a constant supply of external resources to support the energy demands of producing more cells (Delfarah et al., 2019; Glazier, 2015; Marchionni et al., 2020; Stamps, 2007). Long-term energy shortages during growth can have a lasting impact on cellular processes, potentially impairing the organism's functioning over time. One of those biomarkers is the shortening of telomeres (Marasco et al., 2022; Monaghan & Ozanne, 2018; Salmón et al., 2021; Sugimoto, 2014), complexes of DNA repeats and proteins that protect the coding part of the chromosome from incomplete DNA replication (Blackburn et al., 2015). Telomere attrition can be substantial during early growth because of the high rate of DNA replication (Monaghan & Ozanne, 2018; Salmón et al., 2021). Additionally, stressful conditions experienced during the early phases of life can exacerbate telomere attrition (Blackburn & Epel, 2012; Entringer et al., 2011; Epel, 2020). Importantly, early telomere attrition is related to health and life expectancy in animals and humans (Heidinger et al., 2012; Muñoz-Lorente et al., 2019).

The mechanisms underlying telomere erosion in individuals growing under adverse conditions are not fully understood, but a plausible candidate is the activation of the hypothalamus-pituitary-adrenal – 'stress' – axis, which culminates in the secretion of glucocorticoid hormones (Casagrande & Hau, 2019; Giraudeau et al., 2019). When secreted at high concentrations, glucocorticoids bind to the glucocorticoid (GR) receptor. The activation of GR triggers major metabolic changes, including a heightened reliance on internal resources to transform the necessary energy required for the organism to endure the challenge (Chrousos & Kino, 2005; Hau et al., 2016; Yudt & Cidlowski, 2002). Why this process should lead to telomere attrition is a matter of debate. One hypothesis is that glucocorticoids cause oxidative stress (Angelier et al., 2018; Costantini et al., 2011; Picard et al., 2018), where pro-oxidants are produced in excess or cannot be buffered

sufficiently and, consequently, damage vital molecules like DNA and telomeres (Armstrong & Boonekamp, 2023; Reichert & Stier, 2017). However, evidence that physiological concentrations of glucocorticoids cause oxidative stress has not been generally established, as studies on free-ranging birds show (Casagrande & Hau, 2018; Vitousek, Taff, Ardia, et al., 2018). An alternative hypothesis suggests that glucocorticoids shorten telomeres because these hormones can change energy metabolism in a major way ("metabolic telomere attrition hypothesis", Casagrande & Hau, 2019). One cornerstone of the metabolic telomere attrition hypothesis is that telomere length is costly to maintain, and when glucocorticoids signal the need to re-direct limited resources to processes that support immediate survival, telomeres can shorten as a result of this energetic trade-off.

The metabolic telomere attrition hypothesis proposes that glucocorticoids act through specific metabolic pathways, which involve two key components: the mitochondria, where energy is transformed, and the enzyme target of rapamycin (TOR), a sensor of cellular energy supplies that controls growth and metabolism. Growth depends on the availability of resources like energy and specific nutrients (Martin & Hall, 2005; Valvezan & Manning, 2019; Wullschleger et al., 2006). TOR is able to sense the quantities of nutrients and adenosine triphosphate (ATP) available in the cell. If enough resources are present, TOR activates the anabolic pathways needed to grow (Avruch et al., 2009; Betz & Hall, 2013; Limson & Sweder, 2009; N. Zhang et al., 2019) and to maintain long telomeres as observed in yeast, mice and humans (Ferrara-Romeo et al., 2020; Kupiec & Weisman, 2012; Schonbrun et al., 2009; Ungar et al., 2011; Zhou et al., 2003). TOR also receives and integrates different endocrine signals related to energy homeostasis, in order to synchronize energy-consuming processes with energy availability (Kupiec & Weisman, 2012; Martin & Hall, 2005; Schonbrun et al., 2009; Valvezan et al., 2017; Wang & Proud, 2009; Zhang et al., 2019). Specifically, TOR is activated by a positive energetic state, i.e. high levels of nitrogen-rich nutrients, nucleotides, high concentrations of ATP, and by anabolic endocrine signals, for example insulin-like factors, growth hormones and sex steroids (Valvezan & Manning, 2019). When TOR is activated it inhibits catabolic and promotes

anabolic pathways, through specific down-stream signals that lead to the biosynthesis of proteins, lipids and nucleotides (Schieke et al., 2006). Interestingly, an inability to deactivate TOR and thus to curb anabolic processes when nutrients are scarce leads to fatal outcomes, as observed in fasting mice carrying a genetic knockout for the main TOR inhibition pathway (Xu et al., 2014). Inhibition of TOR by nutrient deprivation or hormonal signals activates autophagy to recycle and replenish cellular supplies of vital amino acids and nucleotides (Sudarsanam & Johnson, 2010; Van Leene et al., 2019). Although TOR is a master regulator of cellular metabolism, its main role is the regulation of cell growth when contrasting or rapidly fluctuating signals are present (Ben-sahra et al., 2018; Bonawitz et al., 2007; Dibble & Manning, 2013; Schieke et al., 2006; Valvezan & Manning, 2019). From a more ecological perspective TOR can been seen as a regulator of trade-offs. Glucocorticoids are often viewed to regulate the trade-off between current and future survival (Crespi et al., 2013; Ouyang et al., 2016; Vitousek, Taff, Hallinger, et al., 2018), and the metabolic telomere attrition hypothesis proposes that they could do this by affecting the state of TOR. Exploring this idea may shed some light into the context-dependency of glucocorticoid mediated trade-offs (Breuner et al., 2008).

Nucleotides can influence telomere dynamics also independently from TOR (Figure 1). For instance, the activity of telomerase is influenced by nucleotide levels (e.g. Chen et al., 2018). Recent findings using CRISPR-Cas9 to genetically disrupt nucleotide metabolism pathways in human cultured cells have identified multiple telomere length control points (Mannherz & Agarwal, 2023). Specifically, reducing the salvage or *de novo* production of nucleotides resulted in shortened telomeres, whereas inhibiting nucleotide breakdown enzymes or supplementing with monophosphate nucleotides alone led to significant telomere elongation (Mannherz & Agarwal, 2023). These observations provide strong support for the critical role of nucleotides in telomere maintenance (Casagrande and Hau 2019).

Here we experimentally tested whether the catabolic action of high glucocorticoid concentrations can be counteracted by the effects of high nucleotide availability on telomere dynamics during growth using a wild avian model (*Parus major*, great tit) with known-effects of glucocorticoids on telomere length during a phase of rapid growth (Casagrande et al. 2020). The great tit, is a common passerine found throughout Europe and Asia that has become a popular model species for ecological studies in a variety of research areas (Hau et al., 2022; Laine et al., 2016; Jenny Ouyang et al., 2012; Regan & Sheldon, 2023; Verhagen et al., 2020), including telomere length (Atema et al., 2021; Casagrande et al., 2020; Stier et al., 2016, 2021), mitochondrial (Casagrande et al., 2020; Nord et al., 2021) and gene expression studies (Lindner et al., 2021). Great tits have been found to exhibit substantial variation in telomere length (Atema et al., 2013), which has been linked to various life history traits and environmental factors (Casagrande et al., 2020; Stier et al., 2016, 2021). Here we investigated the combined effects of administration of corticosterone and nucleotides on early-life telomere length. We provided additional nucleotides to free-living great tit nestlings because these can activate TOR (Valvezan & Manning, 2019) and are essential for telomere maintenance in different taxa (Chen et al., 2018; Hoxhaj et al., 2017; Sanford et al., 2021; Valvezan et al., 2017). Moreover, nucleotide shortage impairs cellular division and triggers the replicative stress response. During energy shortages, cells may promote nucleotide salvage pathways rather than, or in addition to, energetically costly new biosynthesis, by allocating recycled nucleotides to the encoding genome (Austin et al., 2012; Casagrande & Hau, 2019). In line with the metabolic telomere attrition hypothesis, we expected that the effect of glucocorticoids on telomere length depends on the energy status of the cells, an information delivered by nucleotides. We therefore predicted that 1) chicks receiving both corticosterone and nucleotides are able to maintain telomere length, as a result of the contrasting effects of nucleotides on the telomere attrition that high concentrations of glucocorticoids cause (Figure 1) (Casagrande & Hau, 2019). We predicted that 2) Nuc-chicks would exhibit longer telomeres than the control group, as nucleotides are expected to be a scarce resource

in this phase of life (Casagrande & Hau, 2019). Specifically, because the positive effects of nucleotides availability on telomere length are directly linked to telomere maintenance processes (Mannherz & Agarwal, 2023) and are not necessarily dependent of the TOR pathway, we expect Nuc-chicks to have longer telomeres than Cnt-chicks (Figure 1). We also expected that longer telomeres are associated with 3) the enhanced expression of telomere maintenance genes (*tert, terf2* and *rap1)* (De Lange, 2005; Epel et al., 2004); 4) a higher expression of the upstream mitochondrial regulator PGC1 (*pprc1*) (Casagrande & Hau, 2019; Sahin & DePinho, 2012); 5) a higher efficiency of mitochondria in coupling aerobic metabolism with ATP production (Casagrande & Hau, 2019; Sahin & DePinho, 2012); 6) a higher expression of mitochondrial complexes involved in the production of ATP (*atp5f1a, atp5f1b, cox6a1, cox4*) (Casagrande & Hau, 2019; Sahin & DePinho, 2012); 7) a lower expression of the kinase AMPK (*prkaa1, prkag3*), which is more abundant when the energetic state of the cell is low (Casagrande & Hau, 2019); 8) higher expression of antioxidant enzymes (*sod1, gpx4*) and total antioxidants (OXY) that protect telomeres from oxidative insults (Armstrong & Boonekamp, 2023; Reichert & Stier, 2017); 9) a lower abundance of oxidative damage (organic peroxides quantified as reactive oxygen metabolites – ROMs) (Armstrong & Boonekamp, 2023; Reichert & Stier, 2017).

To assess the energetic level of the cells we measured the expression of the following genes in the blood: 1. *telo2*, an upstream activator of TOR (Brown & Gromeier, 2017; Fernández-Sáiz et al., 2013; Glatter et al., 2011; Pal et al., 2021) that physically binds to TOR (Glatter et al., 2011). 2. Genes related to telomere length regulation: 2a) Telomerase reverse transcriptase (*tert*), the enzyme that adds nucleotides to telomeres to buffer telomere shortening when cells are dividing (Blackburn, 2001).; 2b) *rap1*, a subunit of the shelterin protein complex that is indispensable for any changes in telomere length, both shortening and elongation (Zhang et al., 2019); 2c) *terf2* subunits of the shelterin protein complex that has a pivotal function in maintaining telomeres in their capped state and preventing their shortening (Ruis et al., 2021). 3) *prkaa1* and *prkag3* (also known as *ampka1* and *ampkg3)* that are adenosine monophosphate kinase (AMPK) subunits. AMPK is activated when ATP

levels are low (Rabinovitch et al., 2017) and deactivates TOR (Martin & Hall, 2005; Seebacher & Little, 2017). 4) *pprc1*, a gene encoding a protein called 'PPARG related coactivator 1', functionally similar to 'PPARG Coactivator 1 Alpha' (also known as PGC-1) according to the GeneCards database (Stelzer et al., 2016). PGC-1 is a master regulator of mitochondrial functioning (Lin et al., 2005; Zhu et al., 2019) able to activate TOR (Cunningham et al., 2007), with potential positive effects on telomere dynamics (Xiong et al., 2015). We also measured 5) mitochondrial traits, specifically 5a) the expression of mitochondrial enzyme subunits of the electron transport chain responsible for the final step of ATP synthesis (cytochrome c oxidase, *cx6a1, cox4*) and subunits of the enzyme that synthesize of ATP (ATP-synthase, *atp5f1a, atp5f1b*); 5b) mitochondrial bioenergetics, specifically cell metabolic rate (CMR) and the proportion of aerobic metabolism allocated to ATP production (OXPHOS), the proportion associated with heat production (LEAK) and calculated indexes of mitochondrial inefficiency (see method section for a definition and description of traits); and 6) oxidative stress status by measuring the expression of 6a) the enzymatic antioxidant genes superoxide dismutase 1 (*sod1*) and glutathione peroxidase 4 (*gpx4*) in red blood cells (RBCs) including in the mitochondria as they encode proteins that convert ROS into hydrogen peroxide (SOD1) and water (GPX4); 6b) extra-cellular biomarkers of oxidative damage (reactive oxygen species metabolites – ROMs) and 6c) oxidative defenses like total non-enzymatic antioxidants (OXY).

Methods

The study was carried out in spring 2017 in a mixed forest located in southern Germany (47°99'N, 11°39'E). One-hundred and fifty nest boxes were checked weekly starting in late March to record the start of incubation, and from day 10 of incubation onwards every other day to record the date of hatching (day 0). After hatching, we randomly allocated nests to two major groups: experimental nests visited every day (n=23) and control nests visited two times (n=10). Experimental and control nests did

not differ in mean (± s.e.m.) clutch size, number of hatchlings or number of fledglings (data published in Casagrande et al. 2020). On day 5 after hatching, we identified the three heaviest nestlings of each brood by weighing them with a digital scale to the nearest 0.1 g. Nestlings from the four groups (Cort- , Nucort-, Nuc- and Cnt-chicks, see below for details) did not differ in body size before the treatment (body mass $F_{(3,47.34)}$=0.81, P=0.49; tarsus length $F_{(3,47.91}$=2.21, P=0.11). Focal chicks were marked with 1–2 yellow or white dots on the skin or feathers of the head with permanent non-toxic markers to allow for quick individual identification. In each experimental nest, the three focal birds were each assigned a different treatment: from day 5 to day 14 Cort-nestlings received daily an oral dose of crystalline corticosterone dissolved in organic peanut oil; NucCort-nestlings received the same oral dose of corticosterone in addition to an oral dose of nucleotides (a mixture of AMP, GMP, CMP and UMP, Chemoforma AG., CH) dissolved in water; Nuc-nestlings received the same dose of nucleotides of NucCort chicks. To maintain the concentration of oral corticosterone at 0.85 µg g^{-1} of body mass and of oral nucleotides at 70 µg g^{-1} of body mass throughout the nestling period, we adjusted the volume of the oral dose to each nestling's body mass measured on days 5, 8 and 12 (range of volumes: 2.3–6.6 µl). The three experimental nestlings in the same nest were therefore exposed to the same levels of disturbance, but differed in their exposure to exogenous corticosterone and nucleotides. Nestlings of control nests (control-nestlings, 3-4 per nest) were handled only 2 times during the nestling period (on days 5 and 15 and a brief visit on day 10 to refresh color markings) and did not receive any treatments. We selected chicks from these nests as controls because handling them daily could trigger the secretion of corticosterone in nestlings (Herborn et al., 2014). This was something we needed to avoid to properly investigate the questions of our study. Therefore, we did not include a group to control for the potential effects of peanut oil. However, our previous study demonstrated that the vector did not play a role in telomere dynamics, mitochondrial bioenergetics, or growth (Casagrande et al., 2020). Some nestlings disappeared from their nest between one visit and the next (control, n=3, Nuc, n=5, NucCort, n=4 Cort, n=3,) while 6 nestlings in control nests lost their colour

marks and were not sampled on day 15. To calculate growth rate, body mass (to the nearest 0.1 g) and tarsus length (to the nearest 1 mm) were recorded on days 5 and 15 in experimental and control nests. All physiological markers considered in the study (see below) were measured for every chick in 80 µl of blood collected with a capillary tube on day 15 by puncturing the ulnar vein, within 3 min of opening the nest box. To minimize any variability due to daily fluctuations of the physiological parameters, nestlings were sampled between 08:00 h and 13:00 h. Blood was immediately stored on ice and within 4 h centrifuged at 2000 g for 10 min; plasma was stored at −80°C and analyzed within 3 months. Red blood cells (RBCs) were washed immediately after sample centrifugation to measure mitochondrial activity as described below (see also Casagrande et al. 2020). An aliquot of RBCs from each individual was stored in newborn calf serum (NBCS) buffer at −80°C until analysis of telomere length. Another aliquot was stored at −80°C until RNA extraction in 2019.

Mitochondrial metabolism analyses

The oxygen consumed by aerobic metabolism during mitochondrial respiration was measured in intact red blood cells (RBCs), which are metabolically active in birds (Engelhardt, 1932; Stier et al., 2013, 2017) following validated protocols (Stier et al., 2017; Casagrande et al. 2020). Briefly, 30 µl RBCs were transferred into 1 ml of cold buffer Mir05 (for details see Casagrande et al. 2020), washed by spinning at 500 x *g* for 5 min and then resuspended in 1 ml of MiR05 buffer already equilibrated at 40°C in a Clark electrode high resolution respirometer (Oxygraph-2k, Oroboros Instruments, Innsbruck, Austria). Mitochondrial respiration was quantified as the O_2 consumed in the following stages: (1) cellular metabolic rate (CMR) – basal respiration of the cells in their natural state; (2) oxidative phosphorylation (OXPHOS) – the process through which ATP is produced - after inhibiting ATP synthase by addition 1 µg ml^{-1} of oligomycin. (3) proton leak (LEAK) -remaining basal respiration that is not affected by oligomycin provided in step 2 and that is uncoupled from ATP production because energy is dissipated in the form of heat. We also measured (4) the working capacity of the electron transport system (ETS)

- by adding the mitochondrial uncoupler carbonyl cyanide m-chlorophenyl hydrazine (CCCP Mitochondria: titration of 1µmol l^{-1} aliquots). The uncoupler causes the flow of electrons through the electron transport system to be independent from the transformation of ADP into ATP. All these traits were corrected for non-mitochondrial O_2 consumption by adding antimycin A (5 µmol l^{-1}), a potent suppressor of mitochondrial metabolism. From these measures we calculated mitochondrial inefficiency to produce ATP in relation to CMR (i.e. proportion of LEAK on CMR: $_{LEAK/CMR}$). All measures were normalized by the volume of RBCs and expressed as pmol O_2*min^{-1}*mL^{-1} of RBCs.

Corticosterone assay

Plasma corticosterone concentrations were determined using an enzyme immunoassay kit (Cat. No. K014-H1; Corticosterone ELISA Kit, Arbor Assays) following a double diethyl ether extraction of a 15 µL plasma sample (for a detailed protocol see (Casagrande et al., 2020)). Samples were re-dissolved in assay buffer and allowed to reconstitute over-night. A buffer blank and two stripped chicken plasma controls (with corticosterone added at concentrations of 10 and 5 ng mL^{-1}, respectively) were taken through the entire procedure. On the next day, 50 µL of each sample (in duplicate) were used. The inter-plate coefficient of variation (CV) was calculated as the average concentration of the four controls (for both high and low concentrations) of the two plates and was 2.40±0.51 %. The intra-plate CV was calculated as the average CV of the concentrations of all the unknown samples run on six plates and was 3.72±0.55 %.

Gene expression analysis

We quantified the expression of 14 genes of interest (*telo2, rap1, terf2, tert, gpx4, sod1, cx6a1, cox4, atp5f1a, atp5f1b, nr3c1, prkaa1, prkag3, pprc1*) relative to a single reference gene (*ube2d2*) (Table) following Casagrande et al. 2020. Briefly, we extracted RNA from RBC samples by mixing 2.5–5 µl

RBCs with 230 µl of TRI Reagent BD (Sigma- Aldrich) and 5 µl of 2.5 M glacial acetic acid and then 60 µl of chloroform. We then centrifuged samples (12,000 g) for 15 min at 4°C, transferred the supernatant to a new tube and added an equal volume of 70% ethanol. This mixture was then applied to a RNeasy column (RNeasy Mini Kit, Qiagen), and followed the standard manufacturer's protocol with a final elution step in 30 µl of EB buffer. We measured RNA concentration and the A260/A280 ratio using a Nanodrop Spectrophotometer (ND-1000) and only samples with an A260/A280 ratio within the range 1.8–2.14 were used. For each sample, we used 400 ng of RNA as a template for cDNA synthesis using the iScript cDNA synthesis kit (Bio-Rad) in a 20 µl reaction according to the manufacturer's instructions. We diluted cDNA 1:10 before use as template in final qRT-PCR assays.

We designed primers for all 14 genes with NCBI Primer-BLAST (Ye et al., 2012). We ensured that each amplicon spanned at least one exon–exon boundary. We ran standard curves to determine the efficiency of primer pairs. We ran standard curves with serially diluted cDNA from a single sample to calculate the amplification efficiency of each primer pair. The serial dilutions we tested were: three dilutions between 1:10 and 1:1000, and if there was no amplification in the 1:1000 dilution a second standard curve was run with 4 four dilutions between 1:10 to 1:100). Efficiency was calculated with the Absolute Quantification tool and 2nd Derivative Maximum method which uses the formula Efficiency=$10^{-1/\text{slope}}$ based on the quantification cycle [Cq, termed crossing point (Cp) in the software] and log concentration of template in each well. The theoretical efficiency of perfect amplification (i.e. exact doubling with each cycle) is 2. The efficiency of primer pairs ranged from 1.909 to 2.07; a detailed summary of standard curve results is listed in Table 3.

We performed qRT- PCR assays across 11 plates with a balanced combination of treatments in each plate. Plates were run in two separate batches: the first batch had four plates and the second batch had seven plates. The first batch contained target genes *nr3c1, prkaa1, prkag3* and *pprc1* and

the second batch contained the remaining target genes listed in Table 3 and Table S3 in the supplementary material. Data for *nr3c1* was previously reported for Cnt and Cort chicks in Casagrande et al., 2020. We ran assays on a LightCycler 480 II (Roche) machine using the SsoAdvanced Universal SYBR Green Super mix (Bio-Rad) in 384-well plates (Roche) and each reaction was run in duplicate. Each well consisted of a 10 µl reaction containing 1× SsoAdvanced Universal SYBR Green Super mix, 340 nmol of each primer and 3 ng of cDNA template (i.e. 1.5 µl of the 1:10 cDNA dilution; the estimate of template amount assumes a one-to-one correspondence between input RNA and synthesized cDNA). The cycling conditions were: pre-incubation step at 95°C for 30 s, 45 cycles at 95°C for 10 s, annealing and extension at 60°C for 30 s, with acquisition at the end of each cycle, followed by a melt curve (95°C for 5 s with 5 acquisitions per °C from 65 to 97°C with a 0.11°C ramp rate). We performed calculations from the raw amplification data using LightCycler 480 software (version 1.5.1.62) and used GraphPad Prism (version 7.05) for additional quality control analyses such as for testing for group differences on reference gene levels and calculating standard curve correlation coefficients. On every plate, we confirmed that each primer pair produced a single melt curve peak in the presence of cDNA template and showed no amplification when water was used as template. In case of primer dimer present in water controls, the melting temperature was clearly distinct from that of the target amplicon and primer dimer was not present in wells with cDNA template. We confirmed that the Cq values for *ube2d2*, pooled from all eleven plates, did not vary among the four treatment groups (Kruskal-Wallis $H(3) = 0.378$, $p = 0.945$; Cq mean±s.e.m.: 21.82±0.25). Expression of target genes was calculated relative to the reference gene *ube2d2* in the software with the Advanced Relative Quantification analysis using the actual primer efficiencies from the standard curve instead of the preassigned value of 2.

Telomere length measure

306 Absolute length of telomeres was measured in RBCs using a non-denaturing terminal restriction
307 fragment (TRF) analysis following (Haussmann & Vleck, 2002). Full details of the protocol used are
308 reported in Casagrande et al. (2020). Briefly, we measured Class II telomere lengths in 5–10 µl RBCs,
309 after DNA extraction with Gentra Puregene Kit (Qiagen). RNA was removed with 2.5 µl RNase.
310 Samples were restriction digested overnight prior to running them on an agarose gel with 0.5× TBE
311 buffer. All samples were run using five gels and analysis was performed singularly because of DNA
312 quantity limitation and because this protocol showed low CV (Stier et al., 2020). Telomere oligos and
313 1kb+ ladder were radio-labelled with 32P. Each reaction was added to Sephadex spin columns and
314 labelled products was stored at 4°C. We used a 0.8% agarose gel for pulsed field electrophoresis. To
315 pre-hybridize the gel, we incubated it at 37°C for 60 min with 50 ml hybridization solution. We then
316 added 50 ml hybridization/ oligo solution to the gel and incubated it overnight, with the same
317 conditions as described in the previous step. The following day, the gel was washed, dried and
318 wrapped in cling film and placed in a phosphor screen cassette for 4 days, then visualized using a
319 Typhoon Variable Mode Imager (Amersham Biosciences). Average telomere length was quantified by
320 densitometry in the program ImageJ (version 2.0) within the limits of our molecular size markers (2–
321 40 kb).
322
323 Oxidative stress
324 Levels of hydroperoxides produced by the oxidation of lipids, proteins and nucleic acids, i.e. reactive
325 oxygen metabolites (ROMs), were quantified with the d-ROM test (Diacron International, Grosseto,
326 Italy; for details see Casagrande et al. 2019 and Casagrande et al. 2020) using a microplate reader
327 (Multiskan Go, Thermo Fisher Scientific, Vantaa, Finland). Measurements are expressed as mmol l^{-1}
328 of H_2O_2 equivalents. All samples, the calibrator and controls for high and low concentrations were
329 run in duplicate. The inter-plate CV was calculated as the average concentration of the four controls

on each of the six plates and was 7.83±3.2%. The intra-plate CV was calculated as the average CV of the concentrations of control samples run on six plates and was 3.18±0.74%.

Plasma non-enzymatic antioxidants were quantified using the OXY-Adsorbent test (Diacron International) Casagrande et al. 2019, 2020) using reference standards and controls for high and low concentrations (all diluted 2:50 with distilled water) or blank (i.e. only water) using a microplate reader (Multiskan Go, Thermo Fisher Scientific). The antioxidant capacity is expressed in µmolHOClml−1. All samples, standards and blank were run in duplicate. The inter-plate CV was calculated as the average concentration of the four controls on each of the six plates and was 15.86±2.26%. The intra-plate CV was calculated as the average CV of the concentrations of control samples run on six plates and was 6.25±1.34%.

Statistical analysis

We obtained data from 69 chicks, but sample sizes differ across variables as some lab assays failed to produce reliable data (see below for further explanations; samples size reported in figures). To assess the effect of the treatments on the variables of interest we ran a model for each response variable with “treatment” as a predictor (4 levels, Cnt, NucCort, Cort and Nuc) and “nest” as a random factor. The assay number, which at first was included as a random factor, was omitted from the models to minimize overfitting and because this information did not change the results (not shown). The effect of the treatments was assessed by model estimates that took as reference group the unmanipulated group (Cnt) in order to assess differences of Cnt chicks to NucCort and Cort chicks, respectively (see above detailed explanations about the use of this group as a valuable control for the questions of the present study). We also provided full pairwise post-hoc comparisons (Tukey’s Bayesian marginal means and 95% CI showed in figures when meaningful; full comparisons reported in Table S2 of the supplementary material).

354 Some variables were highly correlated with each other and were therefore first subjected to a
355 principal component analysis to avoid redundancy. Specifically, we found a strong correlation between
356 mass growth (expressed as the difference in body mass between day 15 and day 5) and tarsus growth
357 (expressed as the difference in tarsus length between day 15 and day 5) ($r=0.61$, $n=69$, $p<0.0001$). The
358 principle component analysis indicated that PC1 explained 80.4% of the variation in growth of both
359 traits and was therefore used in subsequent analyses. The model for growth included initial tarsus
360 length to account for any starting imbalances (initial body mass was not included because of
361 collinearity; see correlation analysis above). For the gene expression analysis, we replaced highly
362 correlated genes with the first principal component factor calculated from a principal component
363 analysis for the following traits: two genes encoding subunits of ATP synthase F1 (*atp5f1a, atp5f1b*,
364 see Table 3 for more specifications) and two genes encoding subunits 4 and 6A1, respectively, of
365 cytochrome c oxidase (*cox4* and *cox6a1*, Table 3; $r=0.58$, $p<0.0001$; PC1 ETC (Electron transport chain)
366 represented 79.20% of the combined traits); *sod1* and *gpx4* (Table 3) ($r=0.48$, $p<0.0001$; PC1
367 represented 73.94% of the combined traits).
368 In order to understand the physiological mechanisms that allowed NucCort birds to maintain
369 relative long telomeres despite the high levels of circulating corticosterone (see results) we ran a
370 linear mixed model to assess which of the traits that responded to the treatment (i.e. *terf2, tert*,
371 PC1ETC, PC1GPX_SODand PC1Growth) predicted telomere length (response variable of the model)
372 with nest as random factor (Table 2). We also included "LEAK" among the predictor because it was
373 enhanced in Cort-chicks but not in NucCort, leading to think that the higher CMR observed in Cort-
374 and NucCort-chicks had two different meanings (i.e. driven by LEAK in Cort and by an enhancement
375 of mitochondrial complexes in NucCort-chicks, see results). We did not include "treatment" to avoid
376 a post-treatment bias as these factors were also the ones that the responded to the treatment
377 (McElreath, 2020). We did not include *telo2*, because it is considered up-stream to TOR activation
378 and, indeed, it was highly correlated with most of the covariates included in the explanatory model

for telomere length (*terf2*, 0.66[0.47,0.85]; *tert*,, 0.38[0.16,0.60]; PC1 ETS, 0.62[0.43,0.81]; PC1 GPX_SOD, 0.52[0.30,0.73]; PC1 growth, -0.20[-0.4,-0.01]; not correlated with leak (0.12[-0.17,0.35]). To run these explanatory models, the missing values caused by random events (i.e. assay failure or insufficient sample volume) were imputed as the mean value of the respective treatment group (see McElreath 2020) (see table SEM1 for statistical comparison between data set with and without missing data computation).

When used as covariates, variables were z-score normalized. We checked whether variables met the assumptions of homogeneity of variance and normal distribution by visually analyzing the graphical distributions of fitted values versus their residuals. Then, all factors were log transformed except for telomere length, non-enzymatic antioxidants OXY and bioenergetics traits (among the latter only ETS was log transformed). All statistical models were fitted using a Bayesian framework implemented in the statistical software R (v. 4.2.2, R Core Team 2022) using the R-package "rstanarm". For all models, we used parameter-flat priors (Korner-Nievergelt et al., 2015). The number of iterations chosen to ensure that the minimum Markov chain Monte Carlo entailed an effective sample size was of 4000 iterations and 4 chains. All models showed absolute autocorrelation values lower than 0.1, satisfied convergence criteria based on the Heidelberger and Welch convergence diagnostics, had an effective sample size ("neff") close to expected iterations, while none had an "rhat" value above 1.0. We drew inferences from the posterior distribution and 95% credible interval (CI), considering fixed effects to be meaningful if the range 2.5-97.5 % CI did not include zero.

Results

Effects of treatment on corticosterone, GR receptor, body size, and telomere length

The main goal of the study was to assess whether additional nutrients could counteract the effects of daily increases in corticosterone concentrations as is typical when stressful conditions occur. Both groups receiving corticosterone, i.e. Cort- and NucCort-chicks, had higher corticosterone concentrations and a higher expression of GR receptor mRNA compared to Cnt-chicks (Table 1; Figure SEM1a,b) and to Nuc (post-hoc difference in corticosterone marginal means: Cort-Nuc: 0.42[0.10,0.75]; NucCort-Nuc: 0.28[-0.01,0.63. Post-hoc difference in GR marginal means Cort-Nuc: 0.61[0.21,1.06]; NucCort-Nuc: 0.38[0.01,0.78]. This result indicates that the treatment was effective in mimicking stressful early life conditions.

Telomere length was shorter only in Cort-chicks (Table 1; Figure 2a), whereas NucCort-birds were able to maintain telomeres at similar length as Nuc- and Cnt-chicks (Post-hoc in Figure 2a). NucCort-chicks and Cort-chicks were smaller at fledging in comparison to controls (95% CI slightly overlapping 0) but were not different from Nuc-chicks, which did not differ from controls (Table 1; Figure 2b).

Effects of the treatments on TOR state and down-stream variables

NucCort-birds had higher gene expression levels of *telo2*, shelterin protein *terf2* (Table 1, Figure 3b) in comparison to all the other groups (Table 1, Figure 3a,b). NucCort had also higher expression of *tert,* but only in relation to Cnt, (Table 1, Figure 3c). NucCort had also a higher expression of genes encoding ATP synthase and cytochrome c oxidase (Table 1, Figure 4a) and antioxidant enzymes GPX and SOD compared to all the other groups (Table 1, Figure 4b). None of the treatments significantly differed from controls in non-enzymatic antioxidants (Table 1, Figure SEM1c) or oxidative damage (Table 1, Figure SEM1d). The treated chicks also did not differ from control chicks for RAP1, AMPK and PGC1 (Table 1, Figure SEM1e-g).

Effects of treatments on mitochondrial bioenergetics

Cort- and NucCort chicks had higher CMR (Table 1, Figure 5a) and a marginally higher ETS (Table 1) while OXPHOS was not different from controls (Table 1, Figure SEM1h,i). Cort had higher levels of CMR also in relation to Nuc, while NucCort CMR did not differ from Nuc (Figure 5a). Only Cort-chicks had a higher LEAK (Table 1, Figure 5b) and consequently a higher mitochondrial inefficiency (calculated as the ratio LEAK/CMR, Table 1, Figure 5c) in relation to controls and NucCort-chicks (see Figure 5b,c for further pair comparisons).

Explanatory model for telomere length

The only parameters that significantly explained telomere length were the gene expression of the respiratory system producing ATP (ATP synthase and COX oxidase expressed by PC1 ETC), which was positively associated with telomere length (Table 2), and LEAK, which was negatively related to telomere length (Table 2). The effects were confirmed when all non-significant predictors were dropped from the model (Table 2).

Discussion

We experimentally tested a core idea of the metabolic telomere attrition hypothesis: that telomere length dynamics are linked to the state of the energy metabolism of an individual (Casagrande & Hau, 2019). Within this framework, we assessed whether the magnified telomere shortage that is often observed when offspring grow up under stressful circumstances (which requires responses that are energetically costly), was counteracted by the availability of sufficient nucleotides. By providing daily oral corticosterone doses to free-living great tit nestlings during their rapid growth phase, we mimicked a protracted exposure to stressful conditions, which did affect their telomere lengths (Casagrande et al. 2020). Specifically, chicks treated with corticosterone alone had the shortest

telomeres while siblings that received a combination of corticosterone and nucleotides were able to maintain their telomere lengths similar to that of the control group. We showed that NucCort chicks were the only group that had a higher gene expression of *telo2*, a proxy for the activation of the enzyme TOR.

Cellular metabolism is inherently a self-regulated process that can proceed independently of TOR. However, when the cell receives contrasting signals, such as increased corticosterone and nucleotide levels, a cellular line of communication within the cell is triggered by TOR to ensure that energy produced in the mitochondria matches energetic needs (Valvezan & Manning, 2019). The need for such a coordination is particularly pressing during the intense cell proliferation that occurs during energetically demanding rapid growth (Wullschleger et al., 2006). Indeed, when only one signal is present, like in Nuc-birds that received additional nucleotides but had low levels of corticosterone, *telo2* expression was not increased (and by extension TOR was not activated). Chicks treated with corticosterone (NucCort- and Cort-chicks) could not maintain growth at the same rate as individuals that were not treated with corticosterone (in Cort-chicks the 95% CI slightly overlapped 0), indicating that the catabolic effects of corticosterone on growth were acting in both groups. In Cort-chicks, where the effect on growth was marginal, it could be speculated that Cort mediated the expected trade-offs between immediate survival (growth) at the expense of long-term benefits represented by telomere lengths. By contrast, NucCort-chick prioritized long-term benefits (telomeres) over short-time benefits (growth), which is puzzling and needs some considerations. Firstly, the enhanced performance of mitochondria observed in NucCort chicks (see explanations about the role of mitochondria below) was not used to boost growth but instead to maintain telomeres, highlighting the importance of limiting telomere loss during this stage of life. Indeed, several studies provide evidence that early telomere attrition constrains future survival (Heidinger et al., 2012; Wood & Young, 2019), likely being the reason why telomere maintenance was prioritized over growth. Secondly, our findings show that growth and telomere downstream pathways are

474 independent processes in this species. TOR is a complex kinase, comprised of several components
475 that can also act independently from each other. For example, Rapamycin is effective in inhibiting
476 the TOR-Complex-1, but not TOR-Complex-2, and the two units have different roles in controlling
477 growth (Cybulski & Hall, 2009). It would be important in the future to investigate the specific
478 pathways that were activated to maintain telomeres in NucCort-birds. This approach would allow to
479 biochemically "visualize" the mechanisms underlining the trade-off between growth and telomere
480 length that is often observed in vertebrates (Geiger et al., 2012; Monaghan & Ozanne, 2018;
481 Spießberger et al., 2022).
482 *Telo2* gene expression, and the related possible activation of TOR, in birds administered with
483 both corticosterone and nucleotides was accompanied by an enhanced functionality of the
484 mitochondria that we observed at several levels. NucCort birds enhanced gene expression of the
485 electron transport system, in particular for genes encoding ATP synthase F1 subunits alpha and beta
486 and cytochrome C oxidase subunits 4 and 6A1, which were positively associated with telomere
487 length. This finding suggests that mitochondria are key elements for telomere dynamics as suggested
488 by the metabolic telomere attrition hypothesis (Casagrande & Hau, 2019). Oxidative phosphorylation
489 is the process through which the mitochondria produce the chemical energy in the form of ATP to
490 fuel anabolic processes in the cell. Indeed, in NucCort-chicks, mitochondrial metabolic rate was
491 enhanced without a concomitant increase in LEAK; indeed, nestlings in this group were more
492 efficient than Cort-chicks in coupling aerobic metabolism with ATP. Since TOR activation depends on
493 sufficient ATP concentrations, this could have further ensured the activated state of TOR. It is also
494 important to consider that mitochondria are not only crucial for ATP production but also for
495 biosynthetic processes. Specifically, they are the core elements in which the biosynthesis of
496 nucleotides takes place. The synthesis of nucleotides in the mitochondria relies on the Krebs cycle
497 (Harrison & Lane, 2018). The rate at which the Krebs cycle runs, in turn, is directly associated with
498 the respiratory function of mitochondria (Lane & Fan, 2015), which could explain why the expression

of genes for respiratory enzymes was the variable that best explained telomere length. In other words, we suggest that a higher mitochondrial efficiency in producing ATP was not only associated with the energy availability of cells but also related to nucleotide synthesis in the mitochondria. Nucleotides are a limiting resource for both telomere maintenance and body growth (Delfarah et al., 2019; Robitaille et al., 2013; Valvezan et al., 2017). They are needed for DNA replication during cell division, as well as the for the RNA required for protein synthesis. Supply of nucleotides is usually guaranteed by salvage pathways that recycle them, but in certain phases like growth, this is not sufficient and their *de novo* synthesis becomes crucial (reviewed in Casagrande and Hau 2019).

Contrary to expectations, we did not find longer telomeres in Nuc-birds, indicating that nucleotides are not a limited resource for these nestlings. Another explanation is that for nucleotides to elongate telomeres independently of TOR, another set of nucleotides should be used, i.e. including thymidine (TMP), which was missing from the mix provided (see methods for further details). A recent study investigating the role of nucleotide metabolism on telomere length in cultured human cells found that thymidine nucleotides are essential for inducing telomere elongation (Mannherz & Agarwal, 2023). In the absence of thymidine, telomeres cannot be elongated even when other nucleotides are fully provided (Mannherz & Agarwal, 2023). This study was published after we conducted our experiment. When we designed our study, we did not actively exclude thymidine from our mix as we had no reason to do so, but unfortunately, it was not commercially available as food additive. Given the recent findings on the importance of thymidine nucleotide for inducing telomere elongation, it is advisable for future studies to pay attention to include thymidine and other key nucleotides when investigating telomere dynamics in similar contexts.

In NucCort-birds, the increase in mitochondrial metabolic rate was paralleled by an upregulation of key antioxidant enzymes that may have prevented oxidative insults caused by a greater production of reactive oxygen species (ROS) due to the increase in mitochondrial metabolic

524 rate (e.g. increase in CMR and ETS observed in NucCort chicks). However, higher mitochondrial
525 metabolic rate is not necessarily associated with higher production of ROS (Koch et al., 2021; Salin et
526 al., 2015; Speakman et al., 2004). Indeed, we also did not find evidence that Cort- and NucCort-birds
527 had higher oxidative damage despite having a high CMR. It is therefore currently unclear why Cort-
528 chicks did not incur oxidative damage as measured by our assays since they did not upregulate
529 enzymatic antioxidants. One possibility is that the inefficiency of mitochondria in linking respiration
530 to oxidative phosphorylation, due to the increase in proton leak, limits the production of reactive
531 oxygen species (uncouple to survival hypothesis; Brand, 2000; Brand et al., 2016; Speakman et al.,
532 2004). Indeed, there is evidence to suggest that corticosterone can be negatively correlated with
533 mitochondrial reactive oxygen species emission (Voituron et al., 2017). It is also relevant to note that
534 antioxidant enzymes were not down-regulated in Cort-chicks, thus we did not find any evidence that
535 corticosterone impaired antioxidant enzymes, as hypothesized to be one reason for why
536 corticosterone can exert pro-oxidant functions (see Angelier et al., 2018; Costantini et al., 2011).
537 We can exclude that Cort treatment acted via AMPK, because gene expression for two
538 subunits (*prkaa1, prkg3)* of this kinase, which is upregulated when ATP is low, did not differ across
539 groups. We can therefore conclude that even though the mitochondria of Cort-chicks were less
540 efficient in producing ATP (because their LEAK also increased), the higher cell metabolic rate induced
541 by corticosterone was likely sufficient in offsetting the inefficiency in producing enough ATP (Picard
542 et al., 2014, 2017, 2018).
543 Gene expression for mRNAs encoding the enzyme that elongates telomeres (TERT) and a
544 protein from the shelterin protein complex (TERF2) were higher in NucCort birds compared to all
545 other groups. The capping state of the telomeres is the critical element that determines cell
546 senescence and thus impaired tissue renewal. Only when telomeres are uncapped because they have
547 become too short, or because shelterin proteins are not adequately produced, they exert their
548 signalling function to promote cellular senescence (Chang et al., 2016; Maï et al., 2020; Pańczyszyn et

549 al., 2020; Ruis & Boulton, 2021). We know very little about the factors that determine the capping
550 state of telomeres, regardless of their length (Timashev & De Lange, 2020), but it is worthwhile to
551 consider that DNA integrity is checked in multiple phases of the cells, not only during cell replication
552 (Chao et al., 2017). This would explain why the expression of shelterin proteins is important for non-
553 replicating red blood cells, the tissue used in our study to measure genes encoding shelterin proteins
554 and other target parameters. Recently, the most comprehensive study on blood-tissue correlations
555 of telomere length in samples from humans of different ages and sex shows that blood telomere
556 length is a proxy for telomere length in 18 tissues out of 23 (associations were not significant for
557 ovary, breast, thyroid, esophagus and coronary tissue) (Demanelis et al., 2020).
558
559 Conclusions
560 We simulated a stressful environment during development by providing daily doses of corticosterone
561 to chicks of a fast-growing bird, showing that the shortening effects of this hormone on telomeres
562 are attenuated when chicks also receive additional nucleotides. This finding suggests that the
563 energetic state of the organism is a crucial factor in the context-dependent actions of glucocorticoids
564 (Jaatinen et al., 2014; Schoenle et al., 2021). We therefore encourage future studies on the effects of
565 glucocorticoids to also evaluate the energetic or nutritional state of individuals. This would be in line
566 with theoretical models formulated to explain the physiological and behavioural outcomes of stress
567 mediators like glucocorticoids - the allostasis model (McEwen & Wingfield, 2003) and the reactive
568 scope model (Romero et al., 2009) - for which the effects of glucocorticoids are not invariant but
569 differ in relation to internal resources and the energy obtainable from the environment. Investigating
570 the complex interactions among different physiological systems as proposed by the metabolic
571 telomere attrition hypothesis – cellular energy availability, mitochondria functioning and metabolic
572 hormones like glucocorticoids – helps us to illuminate some of the pathways connected to telomere
573 maintenance. This is relevant considering that premature cellular aging, caused by early-life telomere

shortening in individuals raised in stressful conditions, can also be observed in human newborns. (Ridout et al., 2018; Send et al., 2017). It is slowly starting to emerge that telomeres are not passive accumulators of damage; rather, they are targeted by several regulatory systems and tightly linked with mitochondrial function (Casagrande & Hau, 2019; Lin & Epel, 2022; Metcalfe & Olsson, 2021). By further investigating the mechanisms that regulate telomere dynamics and their interactions with other cellular systems, we may gain a deeper understanding of their biology.

Ethical statement

All experimental procedures were conducted according to the legal requirements of Germany and were approved by the governmental authorities of Oberbayern, Germany.
All experimental procedures followed the strict ethical and animal welfare guidelines of animal experimentation laws of the European Union (Directive 2010/63/EU), the German Animal Welfare Act and were conducted under the approval of Regierungspräsidium von Oberbayern.

Acknowledgements

We are particularly grateful to Dr. Klaus Hoffmann of Chemoforma AG for providing the pure nucleotides and sharing his knowledge on nucleotide physiology and administration; Prof. Pat Monaghan for sharing her knowledge and facilities for telomere length analysis; Julia Slezacek and Rachele Trevisi for helping in the field and in the lab; and the Evolutionary Physiology group, especially Caro Deimel, for supporting the study.

The present study was funded by the Max Planck Society (to M.H.) and the German Science Foundation (Deutsche Forschungsgemeinschaft – DFG grant CA 1789/1- 1-2017 to S.C.).

Competing interests

The authors declare no competing or financial interests.

Data Accessibility

The data will be publicly accessible upon manuscript acceptance

Author contributions

Conceptualization: S.C., M.H.; Lab analysis: S.C., A.S., M.O., J.L. Formal analysis: S.C.; Data curation: S.C.; Writing - original draft: S.C.; Revision: S.C., M.H. and all co-authors; Project administration: S.C., M.H.; Funding acquisition: S.C., M.H.

References

Angelier, F., Costantini, D., Blévin, P., & Chastel, O. (2018). Do glucocorticoids mediate the link between environmental conditions and telomere dynamics in wild vertebrates? A review. *General and Comparative Endocrinology*, *256*, 99–111. https://doi.org/10.1016/j.ygcen.2017.07.007

Armstrong, E., & Boonekamp, J. (2023). Does oxidative stress shorten telomeres in vivo? A meta-analysis. *Ageing Research Reviews*, *85*(January), 101854. https://doi.org/10.1016/j.arr.2023.101854

Atema, E., Mulder, E., van Noordkijk, A. ., & Verhulst, S. (2013). Ultra-long telomeres mask attrition of short telomeres in great tits Manuscript. *Molecular Ecology Resources*, 0–34.

Atema, Els, van Noordwijk, A. J., & Verhulst, S. (2021). Telomere dynamics in relation to experimentally increased locomotion costs and fitness in great tits. *Molecular Ecology*, *August*, 0–2. https://doi.org/10.1111/mec.16162

Austin, W. R., Armijo, A. L., Campbell, D. O., Singh, A. S., Hsieh, T., Nathanson, D., Herschman, H. R., Phelps, M. E., Witte, O. N., Czernin, J., & Radu, C. G. (2012). Nucleoside salvage pathway kinases regulate hematopoiesis by linking nucleotide metabolism with replication stress. *Journal of Experimental Medicine*, *209*(12), 2215–2228. https://doi.org/10.1084/jem.20121061

Avruch, J., Long, X., Ortiz-Vega, S., Rapley, J., Papageorgiou, A., & Dai, N. (2009). Amino acid regulation of TOR complex 1. *American Journal of Physiology - Endocrinology and Metabolism*, *296*(4), 592–602. https://doi.org/10.1152/ajpendo.90645.2008

Ben-sahra, I., Manning, B. D., & Diseases, C. (2018). mTORC1 signaling and the metabolic control of cell growth. *Curr Opin Cell Biol*, *45*, 72–82. https://doi.org/10.1016/j.ceb.2017.02.012.mTORC1

Betz, C., & Hall, M. N. (2013). Where is mTOR and what is it doing there? *Journal of Cell Biology*, *203*(4), 563–574. https://doi.org/10.1083/jcb.201306041

Blackburn, E. H. (2001). Switching and signaling at the telomere. *Cell*, *106*(6), 661–673. https://doi.org/10.1016/S0092-8674(01)00492-5

Blackburn, E. H., & Epel, E. S. (2012). Telomeres and adversity: Too toxic to ignore. *Nature*, *490*(7419), 169–171. https://doi.org/10.1038/490169a

Blackburn, E. H., Epel, E. S., & Lin, J. (2015). Human telomere biology: A contributory and interactive factor in aging, disease risks, and protection. *Science*, *350*(6265), 1193–1198. https://doi.org/10.1126/science.aab3389

Bonawitz, N. D., Chatenay-Lapointe, M., Pan, Y., & Shadel, G. S. (2007). Reduced TOR Signaling Extends Chronological Life Span via Increased Respiration and Upregulation of Mitochondrial Gene Expression. *Cell Metabolism*, *5*(4), 265–277. https://doi.org/10.1016/j.cmet.2007.02.009

Brand, M. D. (2000). Uncoupling to survive? The role of mitochondrial inefficiency in ageing. *Experimental Gerontology*, *35*(6–7), 811–820. https://doi.org/10.1016/S0531-5565(00)00135-2

Brand, M. D., Goncalves, R. L. S., Orr, A. L., Vargas, L., Gerencser, A. A., Borch Jensen, M., Wang, Y. T., Melov, S., Turk, C. N., Matzen, J. T., Dardov, V. J., Petrassi, H. M., Meeusen, S. L., Perevoshchikova, I. V., Jasper, H., Brookes, P. S., & Ainscow, E. K. (2016). Suppressors of Superoxide-H2O2 Production at Site IQ of Mitochondrial Complex I Protect against Stem Cell Hyperplasia and Ischemia-Reperfusion Injury. *Cell Metabolism*, *24*(4), 582–592. https://doi.org/10.1016/j.cmet.2016.08.012

Breuner, C. W., Patterson, S. H., & Hahn, T. P. (2008). In search of relationships between the acute adrenocortical response and fitness. *General and Comparative Endocrinology*, *157*(3), 288–295. https://doi.org/10.1016/j.ygcen.2008.05.017

Brown, M. C., & Gromeier, M. (2017). MNK inversely regulates TELO2 vs. DEPTOR to control mTORC1 signaling. *Molecular and Cellular Oncology*, *4*(3), 1–2. https://doi.org/10.1080/23723556.2017.1306010

Casagrande, S., & Hau, M. (2018). Enzymatic antioxidants but not baseline glucocorticoids mediate the reproduction–survival trade-off in a wild bird. *Proceedings of the Royal Society B: Biological Sciences*, *285*(1892). https://doi.org/10.1098/rspb.2018.2141

Casagrande, S., & Hau, M. (2019). Telomere attrition: Metabolic regulation and signalling function? *Biology Letters*, *15*(3), 20180885. https://doi.org/10.1098/rsbl.2018.0885

Casagrande, S., Stier, A., Monaghan, P., Loveland, J. L., Boner, W., Lupi, S., Trevisi, R., & Hau, M. (2020). Increased glucocorticoid concentrations in early life cause mitochondrial inefficiency and short telomeres. *The Journal of Experimental Biology*, *223*(June), 222513. https://doi.org/10.1242/jeb.222513

Chang, A. C. Y., Ong, S. G., LaGory, E. L., Kraft, P. E., Giaccia, A. J., Wu, J. C., & Blau, H. M. (2016). Telomere shortening and metabolic compromise underlie dystrophic cardiomyopathy. *Proceedings of the National Academy of Sciences of the United States of America*, *113*(46), 13120–13125. https://doi.org/10.1073/pnas.1615340113

Chao, H. X., Poovey, C. E., Privette, A. A., Grant, G. D., Chao, H. Y., Cook, J. G., & Purvis, J. E. (2017). Orchestration of DNA Damage Checkpoint Dynamics across the Human Cell Cycle. *Cell Systems*, *5*(5), 445-459.e5. https://doi.org/10.1016/j.cels.2017.09.015

Chen, Y., Podlevsky, J. D., Logeswaran, D., & Chen, J. J. (2018). A single nucleotide incorporation step limits human telomerase repeat addition activity. *The EMBO Journal*, *37*(6), 1–17. https://doi.org/10.15252/embj.201797953

Chrousos, G. P., & Kino, T. (2005). Intracellular glucocorticoid signaling: a formerly simple system turns stochastic. *Science's STKE : Signal Transduction Knowledge Environment*, *2005*(304), 1–7. https://doi.org/10.1126/stke.3042005pe48

Costantini, D., Marasco, V., & Møller, A. P. (2011). A meta-analysis of glucocorticoids as modulators of oxidative stress in vertebrates. *Journal of Comparative Physiology B: Biochemical, Systemic, and Environmental Physiology*, *181*(4), 447–456. https://doi.org/10.1007/s00360-011-0566-2

Crespi, E. J., Williams, T. D., Jessop, T. S., & Delehanty, B. (2013). Life history and the ecology of stress: How do glucocorticoid hormones influence life-history variation in animals? *Functional Ecology*, *27*(1), 93–106. https://doi.org/10.1111/1365-2435.12009

Cunningham, J. T., Rodgers, J. T., Arlow, D. H., Vazquez, F., Mootha, V. K., & Puigserver, P. (2007). mTOR controls mitochondrial oxidative function through a YY1-PGC-1α transcriptional complex. *Nature*, *450*(7170), 736–740. https://doi.org/10.1038/nature06322

Cybulski, N., & Hall, M. N. (2009). TOR complex 2: a signaling pathway of its own. *Trends in Biochemical Sciences*, *34*(12), 620–627. https://doi.org/10.1016/j.tibs.2009.09.004

De Lange, T. (2005). Shelterin: The protein complex that shapes and safeguards human telomeres. *Genes and Development*, *19*(18), 2100–2110. https://doi.org/10.1101/gad.1346005

Delfarah, A., Parrish, S., Junge, J. A., Yang, J., Seo, F., Li, S., Mac, J., Wang, P., Fraser, S. E., & Graham, N. A. (2019). Inhibition of nucleotide synthesis promotes replicative senescence of human mammary epithelial cells. *Journal of Biological Chemistry*, *294*(27), 10564–10578. https://doi.org/10.1074/jbc.RA118.005806

Demanelis, K., Jasmine, F., Chen, L. S., Chernoff, M., Tong, L., Delgado, D., Zhang, C., Shinkle, J., Sabarinathan, M., Lin, H., Ramirez, E., Oliva, M., Kim-Hellmuth, S., Stranger, B. E., Lai, T. P., Aviv, A., Ardlie, K. G., Aguet, F., Ahsan, H., … Pierce, B. L. (2020). Determinants of telomere length across human tissues. *Science*, *369*(6509). https://doi.org/10.1126/SCIENCE.AAZ6876

Dibble, C. C., & Manning, B. D. (2013). Signal integration by mTORC1 coordinates nutrient input with biosynthetic output. *Nature Cell Biology*, *15*(6), 555–564. https://doi.org/10.1038/ncb2763

Engelhardt, V. (1932). Die beziehungen zwischen atmung und pyrophosphatumsatz in vogelerythrocyten. *Biochemische Zeitschrift*, *251*, 343–368.

Entringer, S., Epel, E. S., Kumsta, R., Lin, J., Hellhammer, D. H., Blackburn, E. H., Wüst, S., & Wadhwa, P. D. (2011). Stress exposure in intrauterine life is associated with shorter telomere length in young adulthood. *Proceedings of the National Academy of Sciences of the United States of America*, *108*(33). https://doi.org/10.1073/pnas.1107759108

Epel, E. S. (2020). Can childhood adversity affect telomeres of the next generation? Possible mechanisms, implications, and next-generation research. *American Journal of Psychiatry*, *177*(1), 7–9. https://doi.org/10.1176/appi.ajp.2019.19111161

Epel, E. S., Blackburn, E. H., Lin, J., Dhabhar, F. S., Adler, N. E., Morrow, J. D., & Cawthon, R. M. (2004). Accelerated telomere shortening in response to life stress. *Proceedings of the National Academy of Sciences of the United States of America*, *101*(49), 17312–17315. https://doi.org/10.1073/pnas.0407162101

Fernández-Sáiz, V., Targosz, B. S., Lemeer, S., Eichner, R., Langer, C., Bullinger, L., Reiter, C., Slotta-Huspenina, J., Schroeder, S., Knorn, A. M., Kurutz, J., Peschel, C., Pagano, M., Kuster, B., & Bassermann, F. (2013). SCFFbxo9 and CK2 direct the cellular response to growth factor withdrawal via Tel2/Tti1 degradation and promote survival in multiple myeloma. *Nature Cell Biology*, *15*(1), 72–81. https://doi.org/10.1038/ncb2651

Ferrara-Romeo, I., Martinez, P., Saraswati, S., Whittemore, K., Graña-Castro, O., Thelma Poluha, L., Serrano, R., Hernandez-Encinas, E., Blanco-Aparicio, C., Maria Flores, J., & Blasco, M. A. (2020). The mTOR pathway is necessary for survival of mice with short telomeres. *Nature Communications*, *11*(1), 1–17. https://doi.org/10.1038/s41467-020-14962-1

Geiger, S., Le Vaillant, M., Lebard, T., Reichert, S., Stier, A., Le Maho, Y., & Criscuolo, F. (2012). Catching-up but telomere loss: Half-opening the black box of growth and ageing trade-off in wild king penguin chicks. *Molecular Ecology*, *21*(6), 1500–1510. https://doi.org/10.1111/j.1365-294X.2011.05331.x

Giraudeau, M., Angelier, F., & Sepp, T. (2019). Do Telomeres Influence Pace-of-Life-Strategies in Response to Environmental Conditions Over a Lifetime and Between Generations? *BioEssays*, *41*(3), 1–6. https://doi.org/10.1002/bies.201800162

Glatter, T., Schittenhelm, R. B., Rinner, O., Roguska, K., Wepf, A., Jüger, M. A., Köhler, K., Jevtov, I., Choi, H., Schmidt, A., Nesvizhskii, A. I., Stocker, H., Hafen, E., Aebersold, R., & Gstaiger, M. (2011). Modularity and hormone sensitivity of the Drosophila melanogaster insulin receptor/target of rapamycin interaction proteome. *Molecular Systems Biology*, *7*(547). https://doi.org/10.1038/msb.2011.79

Glazier, D. S. (2015). Is metabolic rate a universal “pacemaker” for biological processes? *Biological Reviews*, *90*(2), 377–407. https://doi.org/10.1111/brv.12115

Harrison, S. A., & Lane, N. (2018). Life as a guide to prebiotic nucleotide synthesis. *Nature Communications*, *9*(1). https://doi.org/10.1038/s41467-018-07220-y

Hau, M., Casagrande, S., Ouyang, J. Q., & Baugh, A. T. (2016). Glucocorticoid-Mediated Phenotypes in Vertebrates: Multilevel Variation and Evolution. *Advances in the Study of Behavior*, *48*, 41–115. https://doi.org/10.1016/bs.asb.2016.01.002

Hau, M., Deimel, C., & Moiron, M. (2022). Great tits differ in glucocorticoid plasticity in response to spring temperature. *Proceedings of the Royal Society B: Biological Sciences*, *289*(1986), 14–16. https://doi.org/10.1098/rspb.2022.1235

Haussmann, M. F., & Vleck, C. M. (2002). *Telomere length provides a new technique for aging animals*. *October 2001*, 325–328. https://doi.org/10.1007/s00442-001-0827-y

Heidinger, B. J., Blount, J. D., Boner, W., Griffiths, K., Metcalfe, N. B., & Monaghan, P. (2012). Telomere length in early life predicts lifespan. *Proceedings of the National Academy of Sciences of the United States of America*, *109*(5), 1743–1748. https://doi.org/10.1073/pnas.1113306109

Herborn, K. A., Heidinger, B. J., Boner, W., Noguera, J. C., Adam, A., Daunt, F., & Monaghan, P. (2014). Stress exposure in early post-natal life reduces telomere length: An experimental demonstration in a long-lived seabird. *Proceedings of the Royal Society B: Biological Sciences*, *281*(1782). https://doi.org/10.1098/rspb.2013.3151

Hoxhaj, G., Hughes-Hallett, J., Timson, R. C., Ilagan, E., Yuan, M., Asara, J. M., Ben-Sahra, I., & Manning, B. D. (2017). The mTORC1 Signaling Network Senses Changes in Cellular Purine Nucleotide Levels. *Cell Reports*, *21*(5), 1331–1346. https://doi.org/10.1016/j.celrep.2017.10.029

Jaatinen, K., Seltmann, M. W., & Öst, M. (2014). Context-dependent stress responses and their connections to fitness in a landscape of fear. *Journal of Zoology*, *294*(3), 147–153. https://doi.org/10.1111/jzo.12169

762 Koch, R. E., Buchanan, K. L., Casagrande, S., Crino, O., Dowling, D. K., Hill, G. E., Hood, W. R.,
763 McKenzie, M., Mariette, M. M., Noble, D. W. A., Pavlova, A., Seebacher, F., Sunnucks, P., Udino,
764 E., White, C. R., Salin, K., & Stier, A. (2021). Integrating Mitochondrial Aerobic Metabolism into
765 Ecology and Evolution. *Trends in Ecology and Evolution*, *36*(4), 321–332.
766 https://doi.org/10.1016/j.tree.2020.12.006
767 Korner-Nievergelt, F., Roth, T., von Felten, S., Guélat, J., Almasi, B., & Korner-Nievergelt, P. (2015).
768 The Bayesian and the Frequentist Ways of Analyzing Data. *Bayesian Data Analysis in Ecology*
769 *Using Linear Models with R, BUGS, and STAN*, 19–31. https://doi.org/10.1016/b978-0-12-
770 801370-0.00003-4
771 Kupiec, M., & Weisman, R. (2012). TOR links starvation responses to telomere length maintenance.
772 *Cell Cycle*, *11*(12), 2268–2271. https://doi.org/10.4161/cc.20401
773 Laine, V. N., Gossmann, T. I., Schachtschneider, K. M., Garroway, C. J., Madsen, O., Verhoeven, K. J.
774 F., De Jager, V., Megens, H. J., Warren, W. C., Minx, P., Crooijmans, R. P. M. A., Corcoran, P.,
775 Adriaensen, F., Belda, E., Bushuev, A., Cichon, M., Charmantier, A., Dingemanse, N., Doligez, B.,
776 … Groenen, M. A. M. (2016). Evolutionary signals of selection on cognition from the great tit
777 genome and methylome. *Nature Communications*, *7*, 1–9.
778 https://doi.org/10.1038/ncomms10474
779 Lane, A. N., & Fan, T. W. M. (2015). Regulation of mammalian nucleotide metabolism and
780 biosynthesis. *Nucleic Acids Research*, *43*(4), 2466–2485. https://doi.org/10.1093/nar/gkv047
781 Limson, M. V., & Sweder, K. S. (2009). Rapamycin inhibits yeast nucleotide excision repair
782 independently of Tor kinases. *Toxicological Sciences*, *113*(1), 77–84.
783 https://doi.org/10.1093/toxsci/kfp238
784 Lin, Jiandie, Handschin, C., & Spiegelman, B. M. (2005). Metabolic control through the PGC-1 family
785 of transcription coactivators. *Cell Metabolism*, *1*(6), 361–370.
786 https://doi.org/10.1016/j.cmet.2005.05.004
787 Lin, Jue, & Epel, E. (2022). Stress and telomere shortening: Insights from cellular mechanisms. *Ageing*
788 *Research Reviews*, *73*, 101507. https://doi.org/10.1016/j.arr.2021.101507
789 Lindner, M., Verhagen, I., Viitaniemi, H. M., Laine, V. N., Visser, M. E., Husby, A., & Oers, K. van.
790 (2021). Exploring temporal changes in DNA methylation and RNA expression in a small song
791 bird: correlations within and between tissues. *BMC Genomics*, 1–16.
792 Maï, M. El, Marzullo, M., de Castro, I. P., & Ferreira, M. G. (2020). Opposing p53 and mTOR/AKT
793 promote an in vivo switch from apoptosis to senescence upon telomere shortening in
794 zebrafish. *ELife*, *9*, 1–26. https://doi.org/10.7554/eLife.54935
795 Mannherz, W., & Agarwal, S. (2023). Thymidine nucleotide metabolism controls human telomere
796 length. *Nature Genetics*. https://doi.org/10.1038/s41588-023-01339-5
797 Marasco, V., Smith, S., & Angelier, F. (2022). How does early-life adversity shape telomere dynamics
798 during adulthood? Problems and paradigms. *BioEssays*, *44*(4), 1–11.
799 https://doi.org/10.1002/bies.202100184
800 Marchionni, S., Sell, C., & Lorenzini, A. (2020). Development and Longevity: Cellular and Molecular
801 Determinants-A Mini-Review. *Gerontology*, *66*(3), 223–230.
802 https://doi.org/10.1159/000505327
803 Martin, D. E., & Hall, M. N. (2005). The expanding TOR signaling network. *Current Opinion in Cell*
804 *Biology*, *17*(2), 158–166. https://doi.org/10.1016/j.ceb.2005.02.008
805 McElreath, R. (2020). *Statistical Rethinking in R and STAN*. 612.
806 McEwen, B. S., & Wingfield, J. C. (2003). The concept of allostasis in biology and biomedicine.
807 *Hormones and Behavior*, *43*(1), 2–15. https://doi.org/10.1016/S0018-506X(02)00024-7
808 Metcalfe, N. B., & Olsson, M. (2021). How telomere dynamics are influenced by the balance between
809 mitochondrial efficiency, reactive oxygen species production and DNA damage. In *Molecular*
810 *Ecology*. https://doi.org/10.1111/mec.16150
811 Monaghan, P., & Ozanne, S. E. (2018). Somatic growth and telomere dynamics in vertebrates :
812 relationships, mechanisms and consequences. *Philosophical Transactions of the Royal Society*

B: Biological Sciences, *273*, 20160446.
Muñoz-Lorente, M. A., Cano-Martin, A. C., & Blasco, M. A. (2019). Mice with hyper-long telomeres show less metabolic aging and longer lifespans. *Nature Communications*, *10*(1), 1–14. https://doi.org/10.1038/s41467-019-12664-x
Nord, A., Metcalfe, N. B., Page, J. L., Huxtable, A., McCafferty, D. J., & Dawson, N. J. (2021). Avian red blood cell mitochondria produce more heat in winter than in autumn. *FASEB Journal*, *35*(5), 1–12. https://doi.org/10.1096/fj.202100107R
Ouyang, J. Q., Lendvai, Z., Moore, I. T., Bonier, F., & Haussmann, M. F. (2016). Do Hormones, Telomere Lengths, and Oxidative Stress form an Integrated Phenotype? A Case Study in Free-Living Tree Swallows. *Integrative and Comparative Biology*, *56*(2), 138–145. https://doi.org/10.1093/icb/icw044
Ouyang, Jenny Q., Quetting, M., & Hau, M. (2012). Corticosterone and brood abandonment in a passerine bird. *Animal Behaviour*, *84*(1), 261–268. https://doi.org/10.1016/j.anbehav.2012.05.006
Pal, M., Muñoz-Hernandez, H., Bjorklund, D., Zhou, L., Degliesposti, G., Skehel, J. M., Hesketh, E. L., Thompson, R. F., Pearl, L. H., Llorca, O., & Prodromou, C. (2021). Structure of the TELO2-TTI1-TTI2 complex and its function in TOR recruitment to the R2TP chaperone. *Cell Reports*, *36*(1). https://doi.org/10.1016/j.celrep.2021.109317
Pańczyszyn, A., Boniewska-Bernacka, E., & Goc, A. (2020). The role of telomeres and telomerase in the senescence of postmitotic cells. In *DNA Repair* (Vol. 95). https://doi.org/10.1016/j.dnarep.2020.102956
Picard, M., Juster, R. P., & McEwen, B. S. (2014). Mitochondrial allostatic load puts the “gluc” back in glucocorticoids. *Nature Reviews Endocrinology*, *10*(5), 303–310. https://doi.org/10.1038/nrendo.2014.22
Picard, M., Juster, R. P., Sloan, R. P., & McEwen, B. S. (2017). Mitochondrial Nexus to Allostatic Load Biomarkers. *Psychosomatic Medicine*, *79*(1), 114–117. https://doi.org/10.1097/PSY.0000000000000414
Picard, M., McEwen, B. S., Epel, E. S., & Sandi, C. (2018). An energetic view of stress: Focus on mitochondria. *Frontiers in Neuroendocrinology*, *49*(January), 72–85. https://doi.org/10.1016/j.yfrne.2018.01.001
Rabinovitch, R. C., Samborska, B., Faubert, B., Ma, E. H., Gravel, S. P., Andrzejewski, S., Raissi, T. C., Pause, A., St.-Pierre, J., & Jones, R. G. (2017). AMPK Maintains Cellular Metabolic Homeostasis through Regulation of Mitochondrial Reactive Oxygen Species. *Cell Reports*, *21*(1), 1–9. https://doi.org/10.1016/j.celrep.2017.09.026
Regan, C. E., & Sheldon, B. C. (2023). *Phenotypic plasticity increases exposure to extreme climatic events that reduce individual fitness*. *February*, 2968–2980. https://doi.org/10.1111/gcb.16663
Reichert, S., & Stier, A. (2017). Does oxidative stress shorten telomeres in vivo? A review. *Biology Letters*, *13*(12). https://doi.org/10.1098/rsbl.2017.0463
Ridout, K. K., Levandowski, M., Ridout, S. J., Gantz, L., Goonan, K., Palermo, D., Price, L. H., & Tyrka, A. R. (2018). Early life adversity and telomere length: A meta-analysis. *Molecular Psychiatry*, *23*(4), 858–871. https://doi.org/10.1038/mp.2017.26
Robitaille, A. M., Christen, S., Shimobayashi, M., Cornu, M., Fava, L. L., Moes, S., Prescianotto-Baschong, C., Sauer, U., Jenoe, P., & Hall, M. N. (2013). Quantitative phosphoproteomics reveal mTORC1 activates de novo pyrimidine synthesis. *Science*, *339*(6125), 1320–1323. https://doi.org/10.1126/science.1228771
Romero, L. M., Dickens, M. J., & Cyr, N. E. (2009). The reactive scope model - A new model integrating homeostasis, allostasis, and stress. *Hormones and Behavior*, *55*(3), 375–389. https://doi.org/10.1016/j.yhbeh.2008.12.009
Ruis, P., & Boulton, S. J. (2021). The end protection problem—an unexpected twist in the tail. *Genes and Development*, *35*(1), 1–21. https://doi.org/10.1101/GAD.344044.120
Ruis, P., Van Ly, D., Borel, V., Kafer, G. R., McCarthy, A., Howell, S., Blassberg, R., Snijders, A. P.,

Briscoe, J., Niakan, K. K., Marzec, P., Cesare, A. J., & Boulton, S. J. (2021). TRF2-independent chromosome end protection during pluripotency. *Nature*, *589*(7840), 103–109. https://doi.org/10.1038/s41586-020-2960-y

Sahin, E., & DePinho, R. A. (2012). Axis of ageing: Telomeres, p53 and mitochondria. *Nature Reviews Molecular Cell Biology*, *13*(6), 397–404. https://doi.org/10.1038/nrm3352

Salin, K., Auer, S. K., Rudolf, A. M., Anderson, G. J., Cairns, A. G., Mullen, W., Hartley, R. C., Selman, C., & Metcalfe, N. B. (2015). Individuals with higher metabolic rates have lower levels of reactive oxygen species in vivo. *Biology Letters*, *11*(9). https://doi.org/10.1098/rsbl.2015.0538

Salmón, P., Millet, C., Selman, C., & Monaghan, P. (2021). Growth acceleration results in faster telomere shortening later in life. *Proceedings of the Royal Society B: Biological Sciences*, *288*(1956). https://doi.org/10.1098/rspb.2021.1118

Sanford, S. L., Welfer, G. A., Freudenthal, B. D., & Opresko, P. L. (2021). How DNA damage and non-canonical nucleotides alter the telomerase catalytic cycle. *DNA Repair*, *107*(July), 103198. https://doi.org/10.1016/j.dnarep.2021.103198

Schieke, S. M., Phillips, D., McCoy, J. P., Aponte, A. M., Shen, R. F., Balaban, R. S., & Finkel, T. (2006). The mammalian target of rapamycin (mTOR) pathway regulates mitochondrial oxygen consumption and oxidative capacity. *Journal of Biological Chemistry*, *281*(37), 27643–27652. https://doi.org/10.1074/jbc.M603536200

Schoenle, L. A., Zimmer, C., Miller, E. T., & Vitousek, M. N. (2021). Does variation in glucocorticoid concentrations predict fitness? A phylogenetic meta-analysis. *General and Comparative Endocrinology*, *300*(September), 113611. https://doi.org/10.1016/j.ygcen.2020.113611

Schonbrun, M., Laor, D., López-Maury, L., Bähler, J., Kupiec, M., & Weisman, R. (2009). TOR complex 2 controls gene silencing, telomere length maintenance, and survival under DNA-damaging conditions. *Molecular and Cellular Biology*, *29*(16), 4584–4594. https://doi.org/10.1128/mcb.01879-08

Seebacher, F., & Little, A. G. (2017). Plasticity of performance curves can buffer reaction rates from body temperature variation in active endotherms. *Frontiers in Physiology*, *8*(AUG), 1–8. https://doi.org/10.3389/fphys.2017.00575

Send, T. S., Gilles, M., Codd, V., Wolf, I., Bardtke, S., Streit, F., Strohmaier, J., Frank, J., Schendel, D., Sütterlin, M. W., Denniff, M., Laucht, M., Samani, N. J., Deuschle, M., Rietschel, M., & Witt, S. H. (2017). Telomere length in newborns is related to maternal stress during pregnancy. *Neuropsychopharmacology*, *42*(12), 2407–2413. https://doi.org/10.1038/npp.2017.73

Speakman, J. R., Talbot, D. A., Selman, C., Snart, S., McLaren, J. S., Redman, P., Krol, E., Jackson, D. M., Johnson, M. S., & Brand, M. D. (2004). Uncoupled and surviving: Individual mice with high metabolism have greater mitochondrial uncoupling and live longer. *Aging Cell*, *3*(3), 87–95. https://doi.org/10.1111/j.1474-9728.2004.00097.x

Spießberger, M., Hoelzl, F., Smith, S., Vetter, S., Ruf, T., & Nowack, J. (2022). The tarnished silver spoon? Trade-off between prenatal growth and telomere length in wild boar. *Journal of Evolutionary Biology*, *35*(1), 81–90. https://doi.org/10.1111/jeb.13954

Stamps, J. A. (2007). Growth-mortality tradeoffs and "personality traits" in animals. *Ecology Letters*, *10*(5), 355–363. https://doi.org/10.1111/j.1461-0248.2007.01034.x

Stelzer, G., Rosen, N., Plaschkes, I., Zimmerman, S., Twik, M., Fishilevich, S., Iny Stein, T., Nudel, R., Lieder, I., Mazor, Y., Kaplan, S., Dahary, D., Warshawsky, D., Guan-Golan, Y., Kohn, A., Rappaport, N., Safran, M., & Lancet, D. (2016). The GeneCards suite: From gene data mining to disease genome sequence analyses. *Current Protocols in Bioinformatics*, *2016*, 1.30.1-1.30.33. https://doi.org/10.1002/cpbi.5

Stier, A., Bize, P., Schull, Q., Zoll, J., Singh, F., Geny, B., Gros, F., Royer, C., Massemin, S., & Criscuolo, F. (2013). Avian erythrocytes have functional mitochondria, opening novel perspectives for birds as animal models in the study of ageing. *Frontiers in Zoology*, *10*(1), 1–9. https://doi.org/10.1186/1742-9994-10-33

Stier, A., Delestrade, A., Bize, P., Zahn, S., Criscuolo, F., & Massemin, S. (2016). Investigating how

telomere dynamics, growth and life history covary along an elevation gradient in two passerine species. *Journal of Avian Biology*, *47*(1), 134–140. https://doi.org/10.1111/jav.00714

Stier, A., Hsu, B.-Y., Cossin-Sevrin, N., Garcin, N., & Ruuskanen, S. (2021). From climate warming to accelerated cellular ageing: an 1 experimental study in wild birds 2. *BioRxiv*, 2021.12.21.473625. https://doi.org/10.1101/2021.12.21.473625

Stier, A., Metcalfe, N. B., & Monaghan, P. (2020). Pace and stability of embryonic development affect telomere dynamics: An experimental study in a precocial bird model: Prenatal development affects telomeres. *Proceedings of the Royal Society B: Biological Sciences*, *287*(1933). https://doi.org/10.1098/rspb.2020.1378rspb20201378

Stier, A., Romestaing, C., Schull, Q., Lefol, E., Robin, J.-P., Roussel, D., & Bize, P. (2017). How to measure mitochondrial function in birds using red blood cells: a case study in the king penguin and perspectives in ecology and evolution. *Methods in Ecology and Evolution*, *8*, 1172–1182. https://doi.org/10.1111/2041-210X.12724

Sudarsanam, S., & Johnson, D. E. (2010). Functional consequences of mTOR inhibition. *Current Opinion in Drug Discovery and Development*, *13*(1), 31–40.

Sugimoto, M. (2014). A cascade leading to premature aging phenotypes including abnormal tumor profiles in Werner syndrome (Review). *International Journal of Molecular Medicine*, *33*(2), 247–253. https://doi.org/10.3892/ijmm.2013.1592

Timashev, L. A., & De Lange, T. (2020). Characterization of t-loop formation by TRF2. *Nucleus*, *11*(1), 164–177. https://doi.org/10.1080/19491034.2020.1783782

Ungar, L., Harari, Y., Toren, A., & Kupiec, M. (2011). Tor complex 1 controls telomere length by affecting the level of Ku. *Current Biology*, *21*(24), 2115–2120. https://doi.org/10.1016/j.cub.2011.11.024

Valvezan, A. J., & Manning, B. D. (2019). Molecular logic of mTORC1 signalling as a metabolic rheostat. *Nature Metabolism*, *1*(3), 321–333. https://doi.org/10.1038/s42255-019-0038-7

Valvezan, A. J., Turner, M., Belaid, A., Lam, H. C., Miller, S. K., McNamara, M. C., Baglini, C., Housden, B. E., Perrimon, N., Kwiatkowski, D. J., Asara, J. M., Henske, E. P., & Manning, B. D. (2017). mTORC1 Couples Nucleotide Synthesis to Nucleotide Demand Resulting in a Targetable Metabolic Vulnerability. *Cancer Cell*, *32*(5), 624-638.e5. https://doi.org/10.1016/j.ccell.2017.09.013

Van Leene, J., Han, C., Gadeyne, A., Eeckhout, D., Matthijs, C., Cannoot, B., De Winne, N., Persiau, G., Van De Slijke, E., Van de Cotte, B., Stes, E., Van Bel, M., Storme, V., Impens, F., Gevaert, K., Vandepoele, K., De Smet, I., & De Jaeger, G. (2019). Capturing the phosphorylation and protein interaction landscape of the plant TOR kinase. *Nature Plants*, *5*(3), 316–327. https://doi.org/10.1038/s41477-019-0378-z

Verhagen, I., Tomotani, B. M., Gienapp, P., & Visser, M. E. (2020). *Temperature has a causal and plastic effect on timing of breeding in a small songbird*. https://doi.org/10.1242/jeb.218784

Vitousek, M. N., Taff, C. C., Ardia, D. R., Stedman, J. M., Zimmer, C., Salzman, T. C., & Winkler, D. W. (2018). The lingering impact of stress: Brief acute glucocorticoid exposure has sustained, dose-dependent effects on reproduction. *Proceedings of the Royal Society B: Biological Sciences*, *285*(1882). https://doi.org/10.1098/rspb.2018.0722

Vitousek, M. N., Taff, C. C., Hallinger, K. K., Zimmer, C., & Winkler, D. W. (2018). Hormones and fitness: Evidence for trade-offs in glucocorticoid regulation across contexts. *Frontiers in Ecology and Evolution*, *6*(APR), 1–14. https://doi.org/10.3389/fevo.2018.00042

Voituron, Y., Josserand, R., Le Galliard, J. F., Haussy, C., Roussel, D., Romestaing, C., & Meylan, S. (2017). Chronic stress, energy transduction, and free-radical production in a reptile. *Oecologia*, *185*(2), 195–203. https://doi.org/10.1007/s00442-017-3933-1

Wang, X., & Proud, C. G. (2009). Nutrient control of TORC1, a cell-cycle regulator. *Trends in Cell Biology*, *19*(6), 260–267. https://doi.org/10.1016/j.tcb.2009.03.005

Wood, E. M., & Young, A. J. (2019). Telomere attrition predicts reduced survival in a wild social bird, but short telomeres do not. *Molecular Ecology*, *28*(16), 3669–3680.

https://doi.org/10.1111/mec.15181
Wullschleger, S., Loewith, R., & Hall, M. N. (2006). TOR signaling in growth and metabolism. *Cell*, *124*(3), 471–484. https://doi.org/10.1016/j.cell.2006.01.016
Xiong, S., Patrushev, N., Forouzandeh, F., Hilenski, L., & Alexander, R. W. (2015). PGC-1α Modulates Telomere Function and DNA Damage in Protecting against Aging-Related Chronic Diseases. *Cell Reports*, *12*(9), 1391–1399. https://doi.org/10.1016/j.celrep.2015.07.047
Xu, S., Cai, Y., & Wei, Y. (2014). mTOR signaling from cellular senescence to organismal aging. *Aging and Disease*, *5*(4), 263–273. https://doi.org/10.14336/AD.2014.0500263
Yudt, M. R., & Cidlowski, J. A. (2002). The glucocorticoid receptor: Coding a diversity of proteins and responses through a single gene. *Molecular Endocrinology*, *16*(8), 1719–1726. https://doi.org/10.1210/me.2002-0106
Zhang, N., Meng, Y., Li, X., Zhou, Y., Ma, L., Fu, L., Schwarzländer, M., Liu, H., & Xiong, Y. (2019). Metabolite-mediated TOR signaling regulates the circadian clock in Arabidopsis. *Proceedings of the National Academy of Sciences of the United States of America*, *116*(51), 25395–25397. https://doi.org/10.1073/pnas.1913095116
Zhang, X., Liu, Z., Liu, X., Wang, S., Zhang, Y., He, X., Sun, S., Ma, S., Shyh-Chang, N., Liu, F., Wang, Q., Wang, X., Liu, L., Zhang, W., Song, M., Liu, G. H., & Qu, J. (2019). Telomere-dependent and telomere-independent roles of RAP1 in regulating human stem cell homeostasis. *Protein and Cell*, *10*(9), 649–667. https://doi.org/10.1007/s13238-019-0610-7
Zhou, C., Gehrig, P. A., Whang, Y. E., & Boggess, J. F. (2003). Rapamycin inhibits telomerase activity by decreasing the hTERT mRNA level in endometrial cancer cells. *Molecular Cancer Therapeutics*, *2*(8), 789–795.
Zhu, X., Shen, W., Yao, K., Wang, H., Liu, B., Li, T., Song, L., Diao, D., Mao, G., Huang, P., Li, C., Zhang, H., Zou, Y., Qiu, Y., Zhao, Y., Wang, W., Yang, Y., Hu, Z., Auwerx, J., … Ju, Z. (2019). Fine-Tuning of PGC1α Expression Regulates Cardiac Function and Longevity. *Circulation Research*, *125*(7), 707–719. https://doi.org/10.1161/CIRCRESAHA.119.315529

993 Table 1. Statistical outputs of models used to assess the effect of the treatments on the variables of interest (reference group was the control group).
994 Estimates of fixed (β) and random (σ2) parameters are shown as posterior modes with 95% credible intervals (CI) .
995

Variable (R2)	Fixed effects	β[95% CI]	Random effects	σ^2 [95% CI]
Corticosterone (0.41)				
	Intercept	0.56[0.26,0.86]	nest	0.19[0.01,0.37]
	nuccort	**0.40[0.02,0.75]**		
	cort	**0.54[0.17,0.84]**	residual	0.43[0.34,0.53]
	nuc	0.11[-0.23,0.47]		
GR (0.36)				
	Intercept	-1.02[-1.35,-0.71]	nest	0.22[0.01,0.52]
	nuccort	**0.51[0.05,0.95]**	residual	0.54[0.42,0.68]
	cort	**0.74[0.29,1.22]**		
	nuc	0.12[-0.31,0.59]		
Growth (0.86)				
	Intercept	8.23[6.10,10.26]	nest	0.73[0.47,1.04]
	nuccort	-0.85[-1.61,-0.10]	residual	0.61[0.49,0.78]
	cort	**-0.46[-1.16,0.03]**		
	nuc	-0.38[-1.14,0.38]		
	Tarsusinitial.s	**-0.97[-1.21,-0.73]**		
Telomeres (0.67)				
	Intercept	14.29[13.41,15.17]	nest	0.67[0.21,1.34]
	nuccort	-0.53[-1.63,0.59]		
	cort	**-1.53[-2.62,-0.33]**	residual	0.92[0.71,1.21]
	nuc	-0.58[-1.65,0.55]		
Telo2 (0.21)				
	Intercept	-1.75[-2.01,-1.48]	nest	0.11[0.005,0.34]
	nuccort	**0.65[0.22,1.08]**	residual	0.55[0.45,0.67]
	cort	0.09[-0.34,0.51]		
	nuc	0.18[-0.23,0.58]		
TERF2 (0.59)				
	Intercept	-0.65[-1.1,-0.19]	nest	0.40[0.05,0.72]
	nuccort	**1.02[0.31,1.61]**	residual	0.64[0.49,0.83]
	cort	0.01[-0.59,0.60]		
	nuc	0.21[-0.37,0.79]		
RAP1 (0.17)				

	Intercept	-1.61[-2.10,-1.12]	nest	0.18[0.009,0.51]
	nuccort	0.48[-0.27,0.85]	residual	0.77[0.63,0.95]
	cort	0.41[-0.25,1.04]		
	nuc	0.46[-0.19,1.04]		
TERT (0.15)				
	Intercept	-0.24[-0.57,0.11]	nest	0.14[0.007,0.43]
	nuccort	**0.61[0.09,1.14]**	residual	0.65[0.54,0.81]
	cort	0.32[-0.18,0.82]		
	nuc	0.18[-0.33,0.67]		
GPX_SOD (0.25)				
	Intercept	-0.37[-1.01,0.31]	nest	0.40[0.02,0.97]
	nuccort	**1.10[0.12,2.08]**	residual	1.18[0.93,1.47]
	cort	-0.01[-1.04,0.98]		
	nuc	0.13[-0.75,1.03]		
PC1 ETC (0.23)				
	Intercept	-0.43[-1.19,0.35]	nest	0.35[0.018,0.93]
	nuccort	**1.09[0.01,2.15]**	residual	1.49[1.25,1.87]
	cort	0.13[-1.10,1.32]		
	nuc	-0.21[-1.30,0.9]		
AMPK (0.55)				
	Intercept	-0.89[-1.21,-0.58]	nest	0.27[0.03,0.48]
	nuccort	0.00[-0.42,0.42]	residual	0.45[0.36,0.58]
	cort	-0.18[-0.59,0.24]		
	nuc	-0.12[-0.54,0.32]		
PGC1 (0.09)				
	Intercept	-1.63[-1.87,-1.40]	nest	0.10[0.005,0.29]
	nuccort	0.23[-0.12,0.34]	residual	0.46[0.38,0.57]
	cort	0.11[-0.24,0.46]		
	nuc	0.02[-0.33,0.35]		
CMR (0.41)				
	Intercept	2.59[1.78,3.4]	nest	0.65[0.07,1.23]
	nuccort	**1.05[-0.01,2.15]**	residual	1.31[[1.04,1.64]
	cort	**1.22[0.17,2.31]**		
	nuc	0.38[-0.72,1.42]		
OXPHOS (0.12)				
	Intercept	1.82[1.37,2.27]	nest	0.19[0.010,0.55]

	nuccort	0.46[-0.08,1.01]	residual	0.81[0.66,0.98]
	cort	0.24[-0.35,0.85]		
	nuc	0.00[-0.18,1.08]		
LEAK (0.54)				
	Intercept	0.80[0.27,1.32]	nest	0.47[0.06,0.79]
	nuccort	0.57[-0.13,1.30]	residual	0.79[0.63,1.01]
	cort	**0.97[0.28,1.68]**		
	nuc	0.36[-0.34,1.06]		
ETS (0.59)				
	Intercept	1.5[1.18,1.88]	nest	0.35[0.09,0.56]
	nuccort	**0.45[-0.02,0.90]**	residual	0.47[0.37,0.62]
	cort	**0.41[-0.03,0.84]**		
	nuc	0.13[-0.32,0.58]		
FCR1 (0.38)				
	Intercept	0.30[0.22,0.38]	nest	0.06[0.005,0.11]
	nuccort	0.04[-0.16,0.15]	residual	0.13[0.10,0.16]
	cort	**0.14[0.03,0.25]**		
	nuc	0.09[-0.02,0.19]		
ROMs (0.18)				
	Intercept	-0.08[-0.34,0.18]	nest	0.14[0.006,0.35]
	nuccort	0.03[-0.36,0.40]	residual	0.50[0.41,0.62]
	cort	-0.13[-0.49,0.23]		
	nuc	0.06[-0.33,0.43]		
OXY (0.68)				
	Intercept	208.08[160.58,251.8]	nest	49.56[26.49,75.13]
	nuccort	43.48[-16.17,101.12]	residual	56.77[45.57,73.31]
	cort	23.77[-33.84,80.80]		
	nuc	41.75[-13.81,102.62]		

996

997 Table 2. Explanatory model for telomere length analysis.

Full model					Minimal model				
Variable (R2)	**Fixed effects**	**β[95% CI]**	**Random effects**	**σ^2 [95% CI]**	**Variable (R2)**	**Fixed effects**	**β[95% CI]**	**Random effects**	**σ^2 [95% CI]**
Telomere length (0.68)					**Telomere length (0.69**				
	Intercept	-0.02[-0.27,0.25]	nest	0.58[0.28,0.88]		Intercept	-0.02[-0.27,0.25]	nest	0.60[0.36,0.90]
	ATP_COX	**0.40[0.03,0.77]**	residual	0.72[0.58,0.93]		**ATP_COX**	**0.32[0.12,0.53]**	residual	0.69[0.57,0.88]
	LEAK	**-0.33[-0.56,-0.10]**				**LEAK**	**-0.31[-0.54,-0.09]**		
	Growth	0.16[-0.07,0.39]							
	TERT	0.00[-0.24,0.24]							
	GPX_SOD	-0.05[-0.42,0.30]							
	TERF2	-0.06[-0.32,0.21]							

998

Table 3. Genes and primers

We measured the abundance of 14 genes relative to the reference gene *ube2d2*. Gene accession numbers and corresponding primer sequence are listed. For full details on efficiency of primer pairs see Supplementary Table S3.

Gene	Gene name	Accession number	Primer sequence
ube2d2	ubiquitin conjugating enzyme E2 D2	XM_015641919.1	GTGGTCCCCAGCACTAACTA
			CCGTGCAATCTCAGGCACTA
telo2	telomere maintenance 2	XM_015642370.1	GGTCACACGACAGAAGTGCT
			CACTCTGAGCAACAACGTGC
rap1	terf2 interacting protein	XM_015640049.2	TCGAAAGCACGGAGTCAGAAA
			GAGTCCTCTGGCCCAGTTTT
terf2	telomeric repeat binding factor 2	XM_015640146.1	GCAGCAACACCCGAACATTT
			GGGCTGCCTTTGTGATTCCT
tert	telomerase reverse transcriptase	XM_015618607.2	CTTACAGGTTCCATGCCTGTGT
			CCCATTAACACCCTATACCTGC
gpx4	glutathione peroxidase 4	XM_015651792.1	TTGCTGAGAACTACGGGGTG
			TTTTATTGCATTGCCCAGGGTG
sod1	superoxide dismutase 1	XM_015651740.1	ATCACTGGATTGGCCGATGG
			TGGTGCACCCATTGGTGTTG
cx6a1	cytochrome c oxidase subunit 6A1, mitochondrial (LOC107211853)	XM_015644396.2	GCATCAGGACCAAGCGTTTC
			TTGGGAGAGCGTTAACGTGG
cox4	cytochrome c oxidase subunit 4, isoform 1, mitochondrial (LOC107210061)	XM_015640424.2	ACAAAGGGACAAACGAGTGGA
			GGATGGGGCCGTACATGAAG
atp5f1a	ATP synthase F1 subunit alpha	XM_015653574.1	CAGGGCTGAAGGGTATGTCC
			ACCAGTCCGCTTCACAACAT
atp5f1b	ATP synthase F1 subunit beta	XM_015615638.1	TGAGGGCAACGACTTGTACC
			CAGGGCGACCTTAGAAGTGG
nr3c1	nuclear receptor subfamily 3 group C member 1	XM_015642077.2	GGAATAGGTGCCAGGGATCG
			TTCCAGGGCTTGAATAGCCA
prkaa1	protein kinase AMP-activated catalytic subunit alpha 1	XM_015652899.1	GGGTGAAGATCGGGCACTAC
			AGGCTGCGAATCTTCTGTCG
prkag3	protein kinase AMP-activated non-catalytic subunit gamma 3	XM_015634778.1	TCGTTGTCTTTGACATCTCCCT
			AGCTCTGTGTCTTGCTGTCC
pprc1	peroxisome proliferator-activated receptor gamma, coactivator-related 1	XM_015632930.2	ATGAGACCCTGTCCCCCTTT
			TGTAGGACTCTCGCACTCCA

Figure 1. Basic conceptualization of the study design. Pink pathway represents TOR activation expected for chicks receiving nucleotides and corticosterone while red pathways are for TOR non-activation/inhibition, as expected for Cort-nestlings. Green pathway represents effect of nucleotides on telomere length, independently of TOR. Arrows represent activation while a blunt head arrow represents inhibition. Sharp and blunt-head arrows pointing at telomeres indicate maintenance-elongation or attrition of telomeres, respectively. White circles indicate gene expression (mRNA) for: mitochondrial enzymes of the electron system cytochrome c oxidase (*cox6a1, cox4*); mitochondrial ATP-synthases (*atp5f1a*, *atp5f1b*), mitochondrial and intracellular antioxidants: superoxide dismutase (*sod1*) and glutathione peroxidase (*gpx4*); mitochondrial regulator PGC1 (*pprc1*); telomere maintenance proteins: shelterin proteins (*rap1*, *trf2*) and telomerase (*tert*); biomarker for low energetic state AMPK (*prkaa1, prkag3).* See text for detailed explanations of expectations.

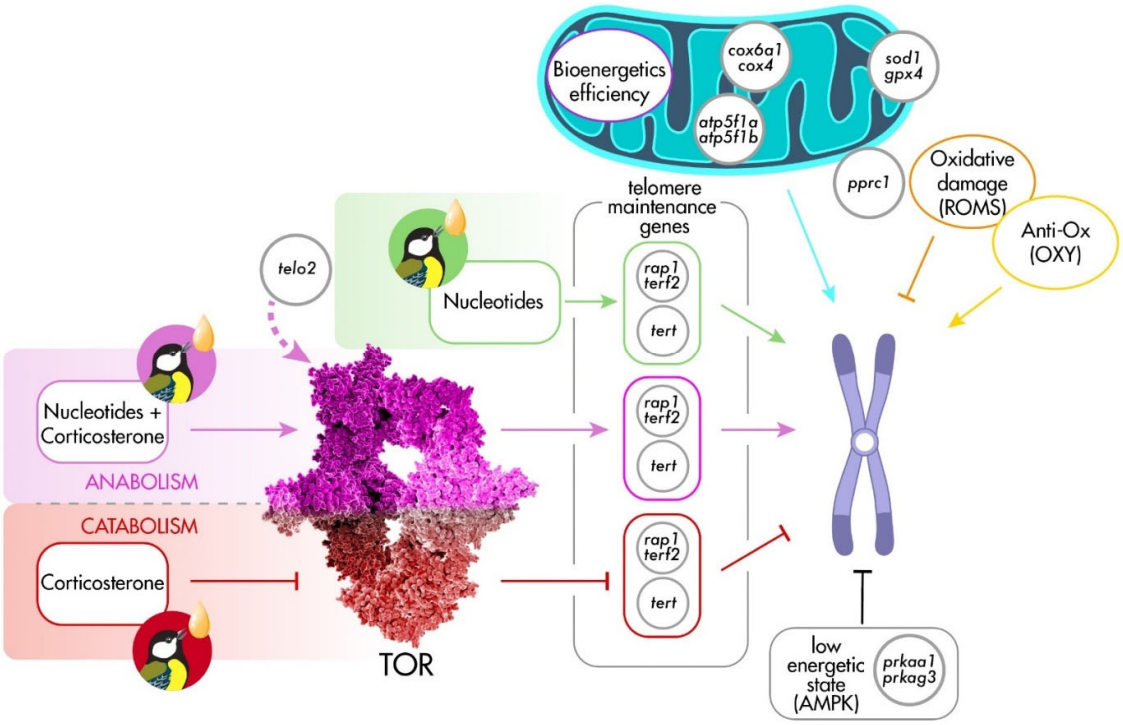

Figure 2. Group differences in telomere length (a) and growth (b). Growth is expressed as the first factor of a PCA including differences between day 5 and day 15 in tarsus length and body mass. Small circles represent individual raw values, while larger circles represent predicted mean values with 95% credible intervals (bars) as calculated by the statistical models. Pairwise Tukey contrasts are reported when between-group differences were significant (missing contrasts indicate lack of significant differences; see SEM for full comparisons). Contrasts were placed above colored lines connecting groups of interest; color refers to the group to which the mean difference was referred.

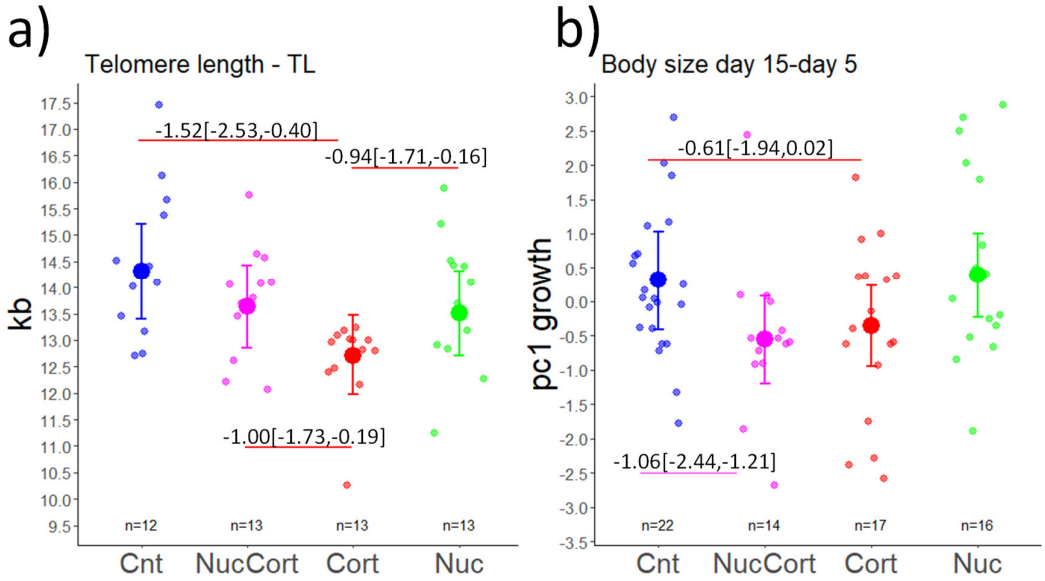

Figure 3. Gene expression of the TOR proxy *telo2,* and telomere maintenance genes *terf2* and *tert*. Small circles represent individual raw values, while larger circles represent predicted mean values with 95% credible intervals (bars) calculated by the statistical models. Contrasts were placed above colored lines connecting groups of interest; color refers to the group to which the mean difference was referred.

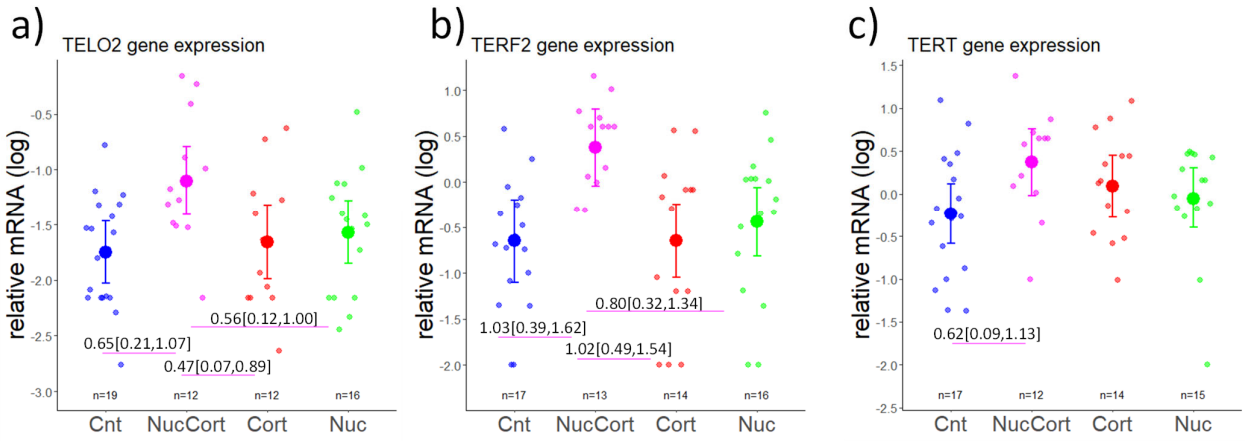

Figure 4. Gene expression of a) 4 subunits of the two mitochondrial enzymatic complexes IV and V (ATP synthase F1 subunits (*atp5f1b,* atp5f1a), cytochrome c oxidase subunits 4 and 6A1 (*cox4, cx6a1*)) expressed by PC1 of a principal component analysis, b) gene expression of two intracellular enzymatic antioxidants (*gpx4*, *sod1)* represent by a PC1 of a principal component analysis (see methods for more details). Pale circles represent individual raw values, while saturated larger circles represent predicted mean values with 95% credible intervals (bars) calculated by the statistical models. Contrasts were placed above colored lines connecting groups of interest; color refers to the group to which the mean difference was referred.

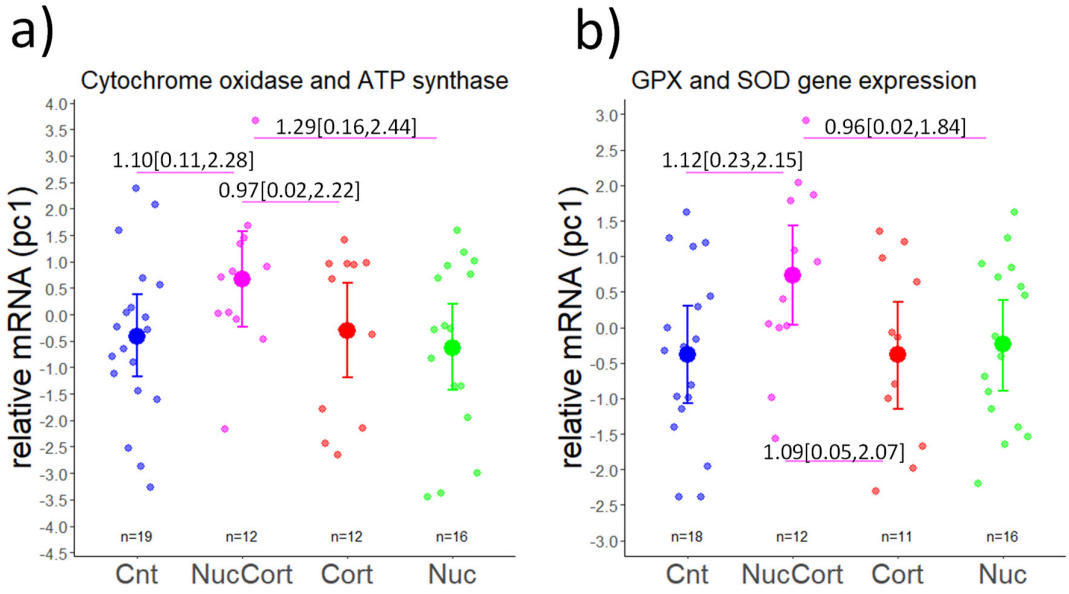

Figure 5. Effect of the treatment on mitochondrial bioenergetics CMR (a), LEAK (b) and mitochondrial inefficiency (c). Pale circles represent individual raw values, while saturated larger circles represent predicted mean values with 95% credible intervals (bars) calculated by the statistical models. Contrasts were placed above colored lines connecting groups of interest; color refers to the group to which the mean difference was referred.

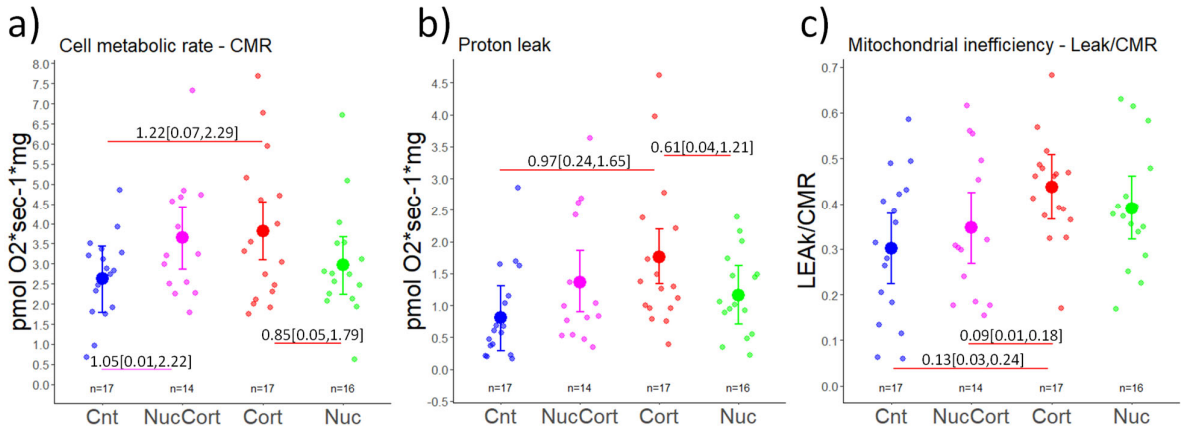

Supplementary material

Table S1. Variation in variables of interest in relation to the treatments (reference group was the control group) with computed missing values. Estimates of fixed (β) and random (σ2) parameters are shown as posterior modes with 95% credible intervals (CI).

Variable (R2)	Fixed effects	β[95% C.I.]	Random effects	σ^2 [95% C.I.]
Telomeres (0.63)				
	Intercept	14.51[13.92,15.06]	nest	0.51[0.12,0.82]
	nuccort	-0.71[-1.45,0.09]		
	cort	**-1.74[-2.43,-1.04]**	residual	0.82[0.67,1.04]
	nuc	-0.76[-1.45,0.06]		
Telo2 (0.23)				
	Intercept	-1.72[-0.97,-1.47]	nest	0.11[0.005,0.32]
	nuccort	**0.66[0.30,1.03]**	residual	0.51[0.43,0.62]
	cort	0.15[-0.21,0.51]		
	nuc	0.14[-0.21,0.51]		
TERF2 (0.66)				
	Intercept	-0.55[-0.98,-0.12]	nest	0.45[0.12,0.73]
	nuccort	**0.91[0.31,1.50]**	residual	0.58[0.46,0.75]
	cort	-0.04[-0.62,0.53]		
	nuc	0.12[-0.45,0.69]		
TERT (0.14)				
	Intercept	-0.13[-0.41,0.17]	nest	0.11[0.007,0.36]
	nuccort	**0.54[0.07,0.98]**	residual	0.62[0.51,0.74]
	cort	0.28[-0.14,0.69]		
	nuc	0.08[-0.34,0.50]		
GPX_SOD (0.23)				
	Intercept	-0.23[-0.82,0.34]	nest	0.34[0.01,0.82]
	nuccort	**1.07[0.23,1.92]**	residual	1.10[0.92,1.35]
	cort	-0.05[-0.74,0.85]		
	nuc	-0.01[-0.83,0.81]		
PC1 ETC (0.17)				
	Intercept	-0.17[-0.88,0.53]	nest	0.34[0.014,0.91]
	nuccort	**1.08[0.01,2.18]**	residual	1.49[1.26,1.82]
	cort	0.26[-0.80,1.30]		
	nuc	-0.44[-1.48,0.6]		
CMR (0.41)				
	Intercept	2.53[1.80,3.22]	nest	0.61[0.05,1.14]
	nuccort	**1.10[0.08,2.14]**	residual	1.27[[1.03,1.58]
	cort	**1.27[0.32,2.31]**		
	nuc	0.43[-0.57,1.44]		

ETS (0.59)				
	Intercept	0.67[0.53,0.81]	nest	0.14[0.04,0.23]
	nuccort	**0.18[-0.01,0.38]**	residual	0.20[0.16,0.26]
	cort	**0.17[-0.01,0.36]**		
	nuc	0.05[-0.13,0.24]		
LEAK/CMR (0.38)				
	Intercept	0.30[0.22,0.38]	nest	0.06[0.004,0.11]
	nuccort	0.05[-0.09,0.15]	residual	0.13[0.10,0.16]
	cort	**0.13[0.04,0.23]**		
	nuc	0.09[-0.02,0.19]		
Growth (0.86)				
	Intercept	8.23[6.10,10.26]	nest	0.73[0.47,1.04]
	nuccort	**-0.85[-1.61,-0.10]**	residual	0.61[0.49,0.78]
	cort	-0.46[-1.16,0.03]		
	nuc	-0.38[-1.14,0.38]		
	Tarsusinitial.s	-0.97[-1.21,-0.73]		

1058

Table S2. Pairwise Post-hoc analysis

$`pairwise differences of treatment`

1	estimate	lower.HPD	upper.HPD
Cnt - NucCort	0.5219	-0.524	1.556
Cnt - Cort	1.5194	0.401	2.526
Cnt - Nuc	0.5669	-0.500	1.588
NucCort - Cort	0.9967	0.190	1.729
NucCort - Nuc	0.0635	-0.662	0.797
Cort - Nuc	-0.9396	-1.705	-0.158

Corticosterone

$`pairwise differences of treatment `

1	estimate	lower.HPD	upper.HPD
Cnt - NucCort	-0.3816	-0.7411	-0.0178
Cnt - Cort	-0.5182	-0.8377	-0.1815
Cnt - Nuc	-0.0967	-0.4246	0.2581
NucCort - Cort	-0.1383	-0.4623	0.1993
NucCort - Nuc	0.2834	-0.0749	0.6285
Cort - Nuc	0.4226	0.1044	0.7486

Gr receptor

$`pairwise differences of treatment `

1	estimate	lower.HPD	upper.HPD
Cnt - NucCort	-0.502	-0.9873	-0.0594
Cnt - Cort	-0.743	-1.2301	-0.2772
Cnt - Nuc	-0.130	-0.6077	0.2882
NucCort - Cort	-0.240	-0.6852	0.1763
NucCort - Nuc	0.371	-0.0377	0.7763
Cort - Nuc	0.613	0.2134	1.0562

Growth pc1

$`pairwise differences of treatment `

1	estimate	lower.HPD	upper.HPD
Cnt - NucCort	1.057	-0.286	2.4395
Cnt - Cort	0.606	-0.740	1.9430
Cnt - Nuc	0.360	-0.998	1.6987
NucCort - Cort	-0.474	-1.138	0.2178
NucCort - Nuc	-0.688	-1.401	-0.0483
Cort - Nuc	-0.224	-0.916	0.4025

Telo2

$`pairwise differences of treatment `

1	estimate	lower.HPD	upper.HPD
Cnt - NucCort	-0.6530	-1.0720	-0.213
Cnt - Cort	-0.0857	-0.5208	0.343
Cnt - Nuc	-0.1718	-0.5828	0.231
NucCort - Cort	0.5602	0.1216	0.996
NucCort - Nuc	0.4721	0.0688	0.888
Cort - Nuc	-0.0873	-0.5039	0.337

Terf2

$`pairwise differences of treatment `

1	estimate	lower.HPD	upper.HPD
Cnt - NucCort	-1.03413	-1.616	-0.387
Cnt - Cort	-0.00914	-0.599	0.607
Cnt - Nuc	-0.21404	-0.774	0.410
NucCort - Cort	1.01583	0.486	1.538
NucCort - Nuc	0.80380	0.322	1.335
Cort - Nuc	-0.20385	-0.711	0.293

Tert

$`pairwise differences of treatment `

1	estimate	lower.HPD	upper.HPD
Cnt - NucCort	-0.619	-1.132	-0.0949
Cnt - Cort	-0.327	-0.849	0.1567
Cnt - Nuc	-0.185	-0.669	0.3052
NucCort - Cort	0.284	-0.252	0.8342
NucCort - Nuc	0.430	-0.103	0.9549

```
 Cort - Nuc        0.146    -0.353    0.6404

Cox
$`pairwise differences of treatment `
 1              estimate lower.HPD upper.HPD
 Cnt - NucCort    -1.098    -2.275     0.103
 Cnt - Cort       -0.110    -1.266     1.010
 Cnt - Nuc         0.206    -0.858     1.300
 NucCort - Cort    0.972    -0.228     2.215
 NucCort - Nuc     1.292     0.155     2.441
 Cort - Nuc        0.330    -0.756     1.502

ATPsynthase
$`pairwise differences of treatment `
 1              estimate lower.HPD upper.HPD
 Cnt - NucCort   -1.1216   -2.1512    -0.226
 Cnt - Cort      -0.0256   -0.9772     1.040
 Cnt - Nuc       -0.1718   -1.0669     0.761
 NucCort - Cort   1.0936    0.0457     2.070
 NucCort - Nuc    0.9609    0.0161     1.840
 Cort - Nuc      -0.1385   -1.0996     0.747

CMR
$`pairwise differences of treatment `
 1              estimate lower.HPD upper.HPD
 Cnt - NucCort    -1.047   -2.2243    0.0114
 Cnt - Cort       -1.218   -2.2869   -0.0708
 Cnt - Nuc        -0.386   -1.4795    0.6774
 NucCort - Cort   -0.175   -1.0953    0.8342
 NucCort - Nuc     0.676   -0.3002    1.6504
 Cort - Nuc        0.853   -0.0586    1.7893

Leak
$`pairwise differences of treatment `
 1              estimate lower.HPD upper.HPD
 Cnt - NucCort    -0.564   -1.2928     0.165
 Cnt - Cort       -0.968   -1.6451    -0.238
 Cnt - Nuc        -0.359   -1.0650     0.309
 NucCort - Cort   -0.406   -1.0235     0.168
 NucCort - Nuc     0.207   -0.4167     0.770
 Cort - Nuc        0.612    0.0351     1.209

Fcr1
$`pairwise differences of treatment
1              estimate lower.HPD upper.HPD
 Cnt - NucCort   -0.0424   -0.1467  0.070024
 Cnt - Cort      -0.1340   -0.2347 -0.030449
 Cnt - Nuc       -0.0867   -0.1926  0.017528
 NucCort - Cort  -0.0911   -0.1846  0.000418
 NucCort - Nuc   -0.0434   -0.1501  0.043345
 Cort - Nuc       0.0478   -0.0412  0.134494
```

Table S3

			Primer design								Standard curve				
Gene	**Primer name**	**Accession number**	**Primer sequence**	**Start**	**End**	**Length**	**Amplicon length**	**Tm(°C)**	**GC(%)**	**Exons spanned**	**Efficiency**	**Error**	**Slope**	**Y-intercept**	**r^2**
ube2d2	FOR*ube2d2*	XM_015641919.1	GTGGTCCCCAGCACTAACTA	276	295	20	100	58.73	55	5 and 6	1.965	0.032	-3.410	18.12	0.99803
	REV*ube2d2*	XM_015641919.1	CCGTGCAATCTCAGGCACTA	375	356	20		60.11	55						
telo2	FOR*telo2*	XM_015642370.1	GGTCACACGACAGAAGTGCT	892	911	20	81	60.25	55.00	6 to 8	1.944	0.0199	-3.463	26.49	0.9752
	REV*telo2*	XM_015642370.1	CACTCTGAGCAACAACGTGC	972	953	20		60.04	55.00						
gpx4	FOR*gpx4*	XM_015651792.1	TTGCTGAGAACTACGGGGTG	386	405	20	131	59.68	55.00	4 and 5	1.981	0.0179	-3.369	23.92	0.98958
	REV*gpx4*	XM_015651792.1	TTTTATTGCATTGCCCAGGGTG	516	495	22		60.03	45.45						
sod1	FOR*sod*1	XM_015651740.1	ATCACTGGATTGGCCGATGG	147	166	20	73	60.18	55.00	2 and 3	1.993	0.0515	-3.340	17.26	0.99695
	REV*sod*1	XM_015651740.1	TGGTGCACCCATTGGTGTTG	219	200	20		61.40	55.00						
cx6a1	FOR*cx6a1*	XM_015644396.2	GCATCAGGACCAAGCGTTTC	324	343	20	78	59.83	55.00	2 and 3	1.955	0.00332	-3.453	18.31	0.99965
	REV*cx6a1*	XM_015644396.2	TTGGGAGAGCGTTAACGTGG	401	382	20		60.32	55.00						
tert	FOR*tert*	XM_015618607.2	CTTACAGGTTCCATGCCTGTGT	3977	3998	22	150	60.55	50	15 and 16	2.079	0.0958	-3.147	22.73	0.99450
	REV*tert*	XM_015618607.2	CCCATTAACACCCTATACCTGC	4126	4105	22		58.25	50						
cox41	FOR*cox41*	XM_015640424.2	ACAAAGGGACAAACGAGTGGA	389	409	21	108	59.79	47.62	4 and 5	1.989	0.0958	-3.348	19.54	0.5118
	REV*cox41*	XM_015640424.2	GGATGGGGCCGTACATGAAG	496	477	20		60.54	60.00						

Figure 1 SEM. Corticosterone administration was effective in increasing circulating levels of the hormone (a) and the gene expression of glucocorticoid receptors (b) in the treated groups NucCort and Cort. For the variables depicted from panel (c) to panel (i) treatment groups did not differ from controls and for this reason were reported here and not in the main text. Pale circles represent individual values, while saturated larger circles represent mean values and 95% credible intervals calculated by the statistical models.